Integrating Hydroacoustic Approaches to Predict Fish Interactions with In-stream Tidal Turbines

Project number: 300-208

Start date: October 1, 2017

Reporting period: October 1, 2017 – December 31, 2019

Recipient name: Fundy Ocean Research Center for Energy (FORCE)

Project lead: Daniel J. Hasselman, FORCE Science Director

Prepared by:
Haley Viehman[1*], Dan Hasselman[2£], Tyler Boucher[2], Jessica Douglas[2], Lindsay Bennett[2]

[1] Echoview Software, Hobart, Tasmania
[2] Fundy Ocean Research Center for Energy, Halifax, NS
*Lead author: haley.viehman@echoview.com
[£]Corresponding author: dan.hasselman@fundyforce.ca

Submission date: December 31, 2019

Table of Contents

1. Executive Summary

A key challenge facing the global marine renewable energy sector is the ability to effectively answer the critical question of the safety of in-steam tidal energy turbines for fish, a key component of the marine environment. Traditional fish sampling technologies, such as trawls, have limited application in high-flow environments. Novel approaches are required to provide the environmental data necessary to achieve public, regulatory, and industry confidence.

FORCE and its partners have been using hydroacoustics to collect information on fish use of the Minas Passage. Two data collection methods have been used: downward-looking, mobile surveys, and upward-looking, stationary surveys. The first method provides spatial coverage of the test site but only spans 24 hours at a time. Conversely, the upward-looking, stationary approach lacks spatial coverage but spans long periods of time (approximately 2 months). There is a need to understand the extent over which results from each survey type might be applied—that is, how much time is represented by the results from a single mobile survey, and how much space is represented by the results from the stationary surveys.

The goal of this project was to use each of these two complementary methods to inform our understanding of the results from the other. Specifically, the mobile acoustic survey data were used to provide an estimate the spatial representative range of the stationary results. The stationary data were be used to estimate the temporal representative range of the 24-hour mobile survey results. Concurrent data collected by the two methods were also compared to assess the challenges associated with each survey type, and to confirm whether both methods provide similar findings.

This assessment utilized backscatter data from repeated passes of one of the mobile transects, and from 3 of the two-month deployments of the stationary platform. The spatial representative range of the stationary results could not be determined using data from the single transect. However, the stationary dataset revealed strong tidal and diel periodicities in volume backscatter (roughly proportional to fish density) at this site, with greater variation occurring at these small time scales than over course of the year. This finding reinforces the importance of 24-hr data collection periods in ongoing monitoring efforts. Collecting at least 24 hours of data at a time allows this tidal and diel variability to be quantified and kept separate from the longer-term trends that we seek to monitor. The temporal representative range of a 24-hr survey was determined to be approximately 3 days. At the 24-hour scale, water column backscatter was comparable across the two survey types, but at shorter time scales, it was not.

Data from both survey types were subject to contamination by backscatter from entrained air in the water column—a common issue at tidal energy sites. All data had to be carefully scrutinized and cleaned, which was an extremely time-consuming process and highlights the need to develop more advanced backscatter classification tools.

2. Introduction and Objectives

The effects of in-stream tidal energy turbines on fish are of high concern to regulators, project developers, fishers, and other members of the public. While we are building our understanding of fish use of high-flow tidal areas, there is still much to be understood in terms of the biology, biophysical linkages, and the methods we are developing to study them. In Nova Scotia, this uncertainty has led to added monitoring requirements at the FORCE tidal test site, but there are limited existing best practices for predicting or detecting in-stream tidal turbine effects on fish and no standard approaches to environmental monitoring.

For an in-stream tidal turbine to affect fish, fish must interact with the device itself or with some part of its physical 'footprint' (e.g., electromagnetic fields, altered hydrodynamics, or acoustic output [1]). To assess the potential for an interaction with any of these components, spatial and temporal patterns in fish distribution in the area where turbine(s) are operating must be understood [2-9]. Though we are building our knowledge of fish use of very fast tidal environments, much remains to be known. In the upper Bay of Fundy, the turnover of species in Minas Channel and Minas Basin is relatively well understood based on studies at weirs and dams in these areas [10,11]. Fish must pass through the Minas Passage to enter or exit the Basin, but information on the presence and distribution of fish within Minas Passage itself is sparse. Data gathered to date indicate that fish presence in the Channel or the Basin does not necessarily reflect that of the Passage [12]. Moreover, fish behavior within the fast currents of the Passage has been found to differ from what is typically expected: Atlantic sturgeon (*Acipenser oxyrhinchus*), a demersal species, were found to traverse the Passage pelagically [3], and Bay of Fundy striped bass (*Morone saxatilis*), previously thought to overwinter in fresh water, were found overwintering within the Passage [2]. Predicting the effects of tidal power development within the Passage – and effectively detecting any – requires a much more thorough understanding of where and when fish are within Minas Passage.

Sampling fish at tidal energy sites is a challenge, as traditional fish sampling techniques (e.g., trawls) are not workable in the fast currents and high turbulence. Hydroacoustics has been identified as one of the more suitable tools for monitoring fish with the necessary resolution and coverage (spatial and temporal) to understand their movements in these dynamic areas [4]. Hydroacoustics refers to sonar technology specialized for observing and monitoring underwater organisms [13,14], and can be used to continuously monitor organisms throughout the water column [4]. This technology has already proven useful for studying fish distribution at tidal energy sites, in a wide range of hydroacoustic survey strategies, e.g. mobile [15-21] or stationary [5,6] vessel-based surveys, and stationary surveys from autonomous [12,16,17,22-25] or shore-connected [26] seabed platforms. Mobile surveys cover large amounts of space, which is essential for understanding how fish and other animals use tidal passages and how likely they may be to encounter in-stream tidal turbines; however, these surveys typically occur over a shorter time period (e.g., one day at a time). In contrast, stationary surveys collect data at one point in space and typically run for a longer period of time (e.g., one month or more), which provides high-resolution records of

how fish presence and vertical distribution at a site vary over short and long time scales [12,22,25-28].

FORCE has been monitoring fish presence and distribution at the test site in Minas Passage using two different hydroacoustic approaches. One is a vessel-based mobile survey, which utilizes a down-facing echosounder to sample fish densities across the test site area [15]. The other is a platform-based, stationary survey, which deploys an echosounder on a bottom-mounted platform for long periods of time [12]. The mobile surveys are meant to track the long-term trends in fish density at the test site, and provide the opportunity to map the spatial distribution of fish in relation to potential locations of turbines. However, these surveys span only 24 hours at a time. The stationary surveys, on the other hand, deploy an autonomous platform on the seafloor to collect acoustic data for up to 2 months at a time, sampling every half hour. These surveys have very good temporal coverage, but only acquire data at one location. Given our limited understanding of fish spatial and temporal distribution at this site, it is unknown how representative the results from either survey are—that is, how much space is represented by readings from the stationary platform, located at one location, and how much time is represented by the short-term measurements from the vessel? A study examining spatially and temporally indexed data in Puget Sound, Washington defined this concept of "representative range" in space and time [16]. That study outlined several approaches to estimating these based on the point at which samples in each dataset cease to remain correlated with themselves. We sought to follow a similar line of investigation at the FORCE site, using spatial and temporal correlation metrics to understand the potential reach of each survey method. The specific questions we sought to answer were,

1. What is the spatial representative range of hydroacoustic data collected at one location in the FORCE test site?
2. What is the temporal representative range of hydroacoustic data collected over a short period of time at the FORCE test site?
3. Are concurrent results from the mobile and stationary datasets comparable to each other, and how did challenges differ across methods?

Integrating these two approaches to answer these questions will allow for a better understanding of fish use of the site, which will inform probability of encounter models in future [19]. The information gained through this integrated approach and evaluation of the strengths and weaknesses of each survey method will additionally inform recommendations of best practices for monitoring turbine effects.

3. Methodology

Hydroacoustic surveys of the FORCE site have been ongoing since 2016. This project utilized data collected by two main survey methods from December 2017 to November 2018, during which time several of the 24-hr mobile surveys overlapped with the long-term stationary data collection from the bottom-mounted platform (Table 1).

Table 1. Summary of overlapping stationary platform deployments and mobile vessel-based surveys.

Platform deployments (stationary)			**Vessel surveys (mobile)**	
Start date	**End date**	**Location**	**Start date**	**End date**
14 Dec 2017	22 Feb 2018	45˚21'46.8" N 64˚25'39.7" W	15 Feb 2018	16 Feb 2018
30 Mar 2018	23 May 2018	45˚21'47.3" N 64˚25'38.9" W	10 Apr 2018	11 Apr 2018
			08 May 2018	09 May 2018
15 Sep 2018	13 Dec 2018 (Data collected until 19 Nov 2018)	45˚21'47.5" N 64˚25'39.9" W	20 Sep 2018	21 Sep 2018
			21 Oct 2018	22 Oct 2018

Mobile vessel surveys were carried out as described in [15]. The stationary platform was deployed in the same area, close to transect 4 of the mobile surveys (Figure 1). For this reason, data from transect 4 were used in these analyses.

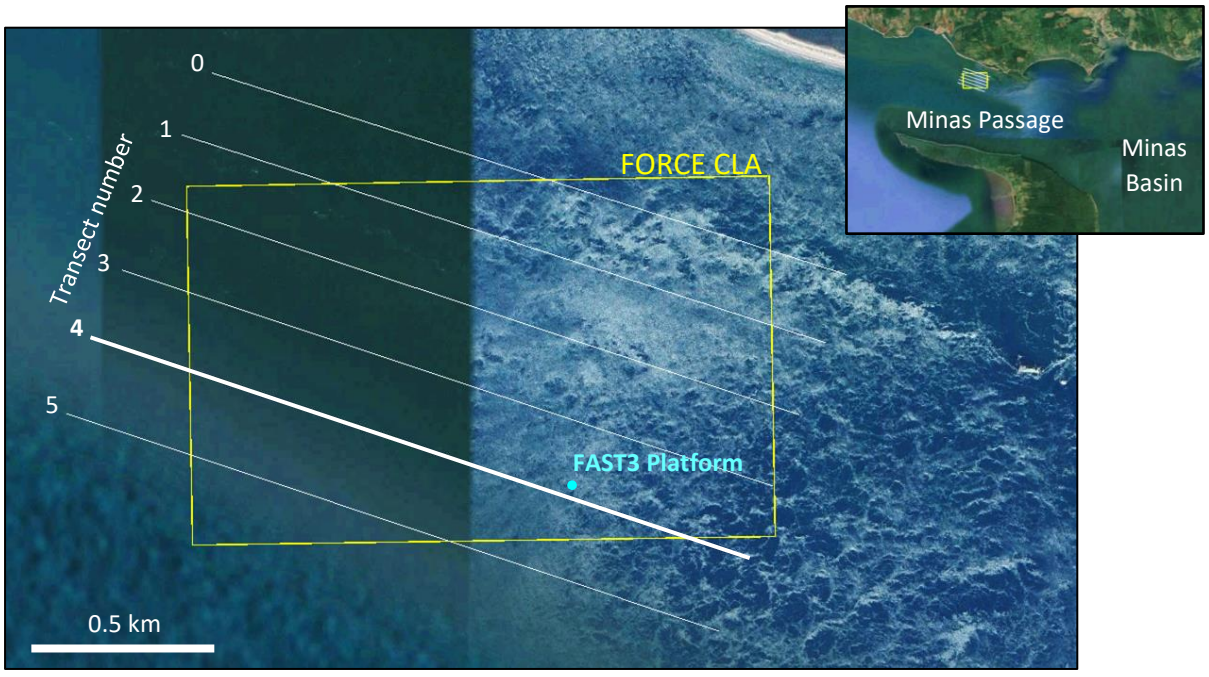

Figure 1. Stationary and mobile hydroacoustic survey locations at the FORCE crown lease area (CLA) in Minas Passage.

3.1. Mobile vessel surveys

The details relevant to this project are reviewed here, but full details may be found in the [15].

Transects were carried out aligned as closely as possible with the lines shown in Figure 1, which formed the northern grid of the survey. The vessel would sample this grid and another on the southern side of the passage once during each tidal stage, resulting in sampling each stage (ebb and flood) at each grid once during the day and once during the night. Each transect was repeated twice, with the vessel travelling with the current in one pass and against the current in the other.

Only data from transect 4 were used in this assessment, as this transect was closest to the FAST3 stationary platform (~40 m closest distance). All surveys were carried out on the neap tide in order to reduce variability related to the lunar cycle, as well as to reduce the detrimental effect of current speed on data quality.

The vessel was equipped with a Simrad EK80 WBT echosounder, with a 7˚ circular split-beam transducer mounted on a pole over the side and oriented downward. This echosounder pinged 2 times per second, at a frequency of 120 kHz (narrowband, “CW mode”) with a pulse duration of 1.024 ms and power output of 250 W.

Calibrations were carried out before each survey by suspending a 23 mm copper calibration sphere on monofilament line at least 2 m below the transducer face [29]. This was carried out at high tide while the vessel was dockside, prior to each survey [15].

3.2. Stationary platform deployments

This project utilised the Fundy Advanced Sensor Technology platform, FAST3 (Figure 2). This platform was equipped with two echosounders: a Simrad EK80 Wideband Autonomous Transceiver (WBAT), and an ASL Environmental Sciences Acoustic Zooplankton Fish Profiler (AZFP). The platform also included a Nortek Signature 500 ADCP and an Aanderaa SeaGuard Recording Current Meter (RCM). The WBAT, AZFP, and Signature 500 were operated in alternating intervals to avoid acoustic contamination across instruments. This project used acoustic data from the Simrad WBAT, and “auxiliary” data from the Signature 500 and RCM, as described in more detail below.

Figure 2. FAST3 platform prior to deployment at the FORCE test site. (a) ASL AZFP transducer; (b) Aanderaa SeaGuard RCM; (c) Nortek Signature 500; (d) Simrad EK80 WBAT transducer.

3.2.1. Simrad EK80 WBAT

The Simrad EK80 WBAT transducer was mounted to the platform with its face at 0.7 m height, facing upward. The transducer had a circular beam with a half-power beam angle of 7˚. It operated at 120 kHz (narrowband, CW mode), with a nominal pulse duration of 0.128 ms, a ping rate of 1 Hz, and a power output of 125 W. The data collection range was limited to 60 m to reduce the required storage capacity and allow longer deployments. Data were collected for 1 minute in passive mode and 5 minutes in active mode every half-hour for the duration of each platform deployment. Passive data were collected to monitor system noise during the deployment, but were not used in the analyses presented here.

Calibration data were collected with the WBAT between deployments, on 6 March 2018 and 13 July 2018. These data were collected *ex situ* at the Dominion Diving wharf in Dartmouth, Nova Scotia, due to difficulty in positioning the sphere within the beam at the deployment location, where the water is constantly moving. Readings were obtained of a standard 23 mm copper calibration sphere was suspended at least 2 m below the transducer face [29]. Data were collected with the same settings used during deployments, and salinity and temperature during calibration were measured separately. Calibration data processing is described in section 3.3.1.

3.2.2. Nortek Signature 500 ADCP

The Nortek Signature 500 ADCP was mounted to the platform, facing upward, similarly to the WBAT transducer. This instrument sampled the water column for a 5 min period of time, every 15 minutes in the Dec 2017-Feb 2018 and Mar-May 2018 deployment, and every 30 minutes in the Sep-Nov 2018 deployment. The sample rate during each burst was 4 per second in Dec-Feb and Sep-Nov deployments, and 2 per second in the Mar-May deployment.

3.2.3. Aanderaa SeaGuard RCM

The Aanderaa SeaGuard RCM measured conductivity, temperature, turbidity, pressure, current speed, and current direction at the platform each half hour for all deployments except September 2018, when the instrument was not operational.

3.3. Hydroacoustic data Processing

Acoustic data collected at tidal energy sites require a large amount of processing prior to analysis. This is mainly due to the large quantities of air entrained into the upper water column by current-, wind-, and wave-induced turbulence, sometimes extending to the sea floor at this site. Data processing was carried out in Echoview® software (10.0, Myriax, Hobart, Australia), and consisted of calibration, noise removal, data partitioning, and echo integration.

Volume backscatter (S_V) data were used in these analyses. S_V is the total sound energy backscattered at a given range and normalized to a unit volume of water, and has units of dB re 1 m^2m^{-3}. S_V can be used as a rough index of fish density (though note that this is confounded by the different scattering properties of individual fish related to species, size, and orientation relative to the transducer) [13, 30].

3.3.1. Data calibration

Calibration parameters obtained from in- and ex-situ calibration data collection methods (sections 3.1 and 3.2.1) were applied to the data. These parameters included direct backscatter corrections (gain and Sa correction), as well as corrections for the environmental conditions experienced by the echosounder during data collection (e.g., temperature and salinity, which determined absorption coefficient, sound speed, and the corresponding adjustments to equivalent beam angle) [29].

For the mobile surveys, surface water temperature was measured from the vessel during each transect, and salinity was measured several times throughout the day via refractometer. The average temperature recorded for transect 4, and the average salinity for each survey, were used to calibrate the data used here (Table 2, Figure 3). Measurements from the stationary platform revealed tidal variation in sound speed, meaning using a daily average sound speed could introduce error to acoustic backscatter values. However, this potential error was quite low (see below), and unlikely to affect the analyses presented here.

Table 2. Summary of environmental parameters during each mobile vessel survey. Sound speed was calculated using equations in references indicated.

Start date	End date	Temperature (˚C)	Salinity (ppt)	Sound speed ($m \cdot s^{-1}$)
15 Feb 2018	16 Feb 2018	0	36	1451.5 [31]
10 Apr 2018	11 Apr 2018	2.7	36	1463.1 [32]
08 May 2018	09 May 2018	6.3	35	1476.7 [32]
20 Sep 2018	21 Sep 2018	15	33	1505.1 [32]
21 Oct 2018	22 Oct 2018	11.5	35	1495.9 [32]

The stationary datasets spanned approximately 2 months each and experienced a far greater range of environmental condition than each 24-hour mobile survey. The stationary

dataset therefore required a different approach to determining environmental parameters for calibration. Sound speed could change by as much as 36 $m \cdot s^{-1}$ from the start of a deployment to the end (Figure 3; see section 3.4.2 for calculations). As sound speed is used in the calculation of backscatter values, one value could not be used for an entire deployment. Sound speed could vary by as much as +/- 4.5 $m \cdot s^{-1}$ over the course of a tidal cycle due to changes in temperature (primarily) and salinity, which correlates to approximately +/- 2.5% error in volume backscatter. To keep backscatter error within the bounds of this tidal variation, the stationary acoustic datasets were split whenever the cumulative change in the 12-hr average sound speed exceeded 4.5 $m \cdot s^{-1}$ (Figure 3). The average temperature, salinity, sound speed, and absorption coefficient were calculated for and applied to each of these data subsets, and used to correct the equivalent beam angle from its factory value [29].

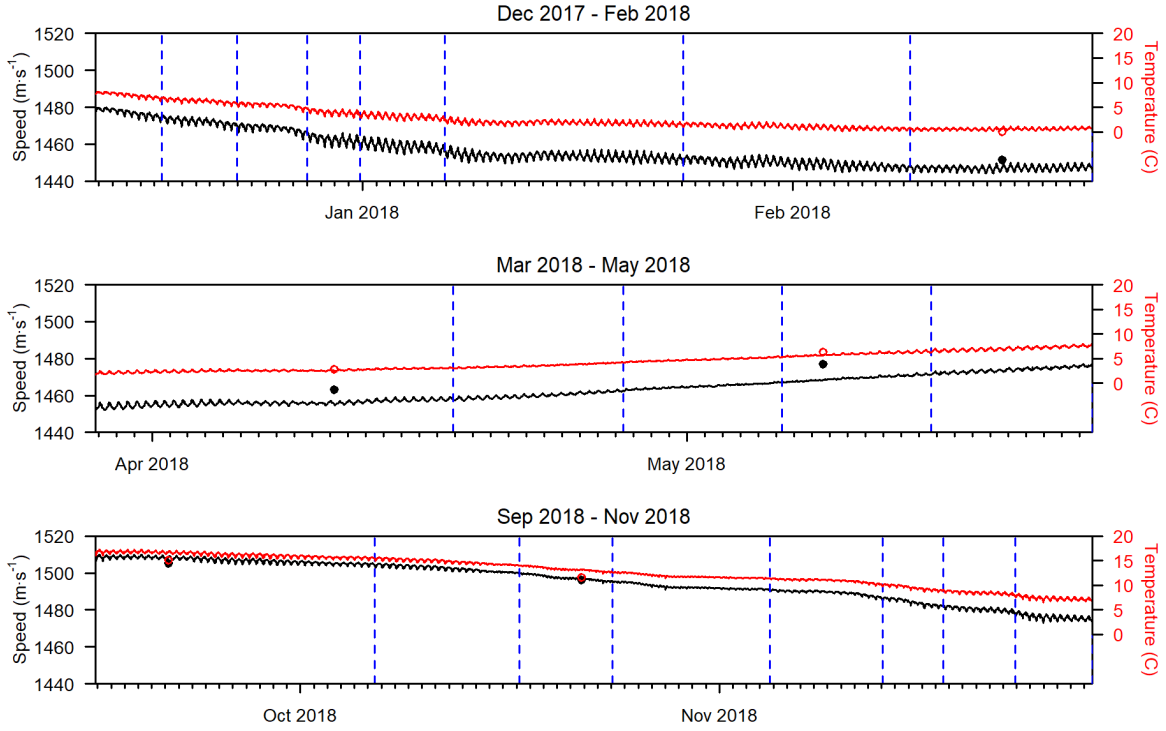

Figure 3. Sound speed and temperature used to calibrate stationary (lines) and mobile (points) acoustic data. Black indicates sound speed and red indicates temperature. Vertical dashed lines indicate calibration subsets of the stationary datasets.

The vessel-based measurements of salinity and temperature differed slightly from the simultaneous platform measurements (Figure 3), and therefore sound speed values were somewhat different for the mobile and stationary datasets, particularly for the April and May mobile surveys. This difference could be related to the different instruments and conversion factors in use, or potentially to differences in surface- and bottom-water parameters (though the water column is generally well-mixed). Direct comparisons of measurements of the same volume of water by each instrument would be helpful in determining the source of this difference in future.

The other necessary Simrad calibration parameters, gain and S_a correction, were calculated for each dataset using Echoview software, measurements of the standard calibration sphere (collected as described in section 3.2.1), and equations from [29].

3.3.2. Noise removal

Once data were calibrated, a minimum S_V threshold of -70 dB re 1 m^2 m^{-3} was applied in both the mobile and stationary datasets. This threshold removed backscatter from weak acoustic targets, more likely to be from non-fish targets (e.g. zooplankton, debris, sediment, and low-amplitude "background" noise). Any remaining unwanted backscatter was then identified and removed. This unwanted backscatter included backscatter from within 2x the transducer's nearfield (calculated to be 1.4 m) [14,29], the bottom (down-looking data collection) or surface (up-looking data collection), several types of distinct water column artefacts, and what we are describing as "transient noise," similar in appearance to that described in [33]. More detail on each type of noise and how it was removed is provided below.

3.3.2.1 Surface and bottom

Echoview's bottom detection algorithm was used in both datasets to detect the surface (stationary, up-looking dataset) or bottom (mobile, down-looking dataset). The algorithm parameters were optimized by eye, and any necessary corrections were applied manually.

3.3.2.2 Entrained air

A threshold offset line was used to delineate the lower limit of the entrained air extending downward from the surface in each dataset (Figure 4). Prior to line detection, the data were blurred somewhat with a 13 sample x 13 ping convolution, which enhanced the entrained air backscatter and made the threshold detection line more effective at removing air backscatter near the edges of the plumes. The entrained air line was then manually edited to ensure it removed as much backscatter from entrained air, and as little backscatter likely to be from fish, as possible.

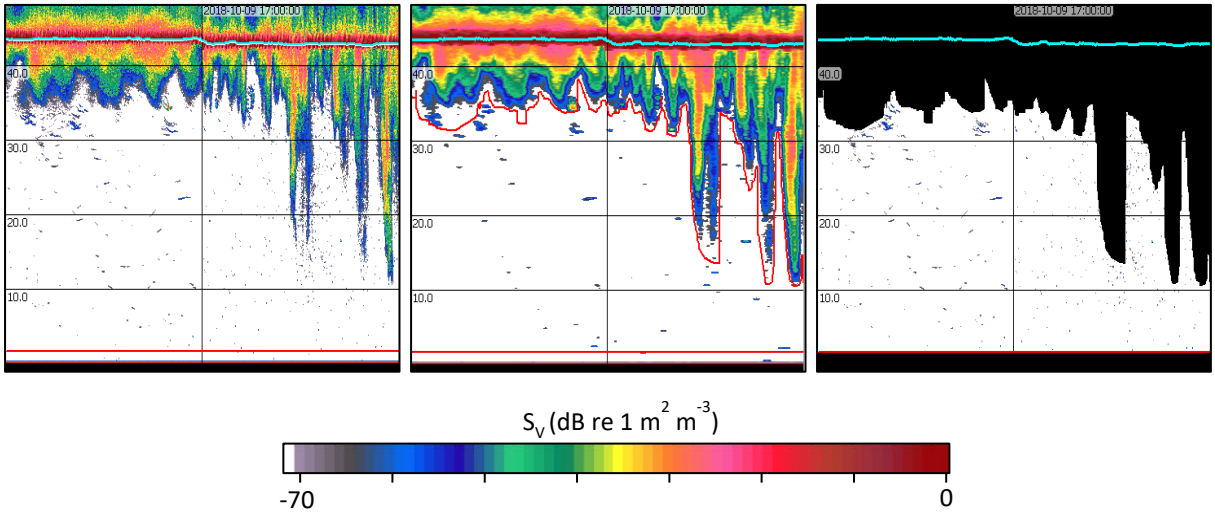

Figure 4. Detection and removal of entrained air from S_V data from the stationary dataset. Left: original S_V data, showing the nearfield (flat red line) and detected surface (thick cyan line). Middle: 13x13 convolution filter of original data, with threshold offset line delineating the entrained air (upper red line). Right: original S_V data with entrained air, nearfield, and surface backscatter removed.

3.3.2.3 Distinct water column artefacts

Several visually distinct acoustic signals, unlikely to be from fish, were present in the data and had to be manually removed. These were:

a) *Interference from other acoustic instruments*. This noise typically appeared as individual contaminated pings, or a few in a row, and most often was likely due to a vessel passing nearby (Figure 5). It occurred rarely and was removed manually by defining bad data (no data) regions.

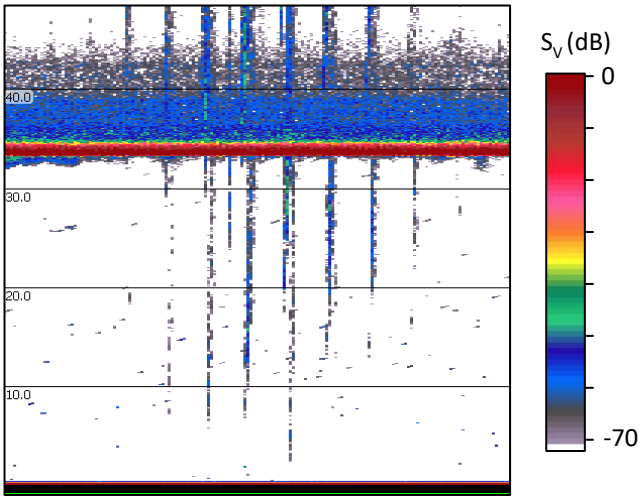

Figure 5. Example of acoustic interference from vessel echosounder in stationary dataset.

b) *Very strong backscatter*. In the stationary dataset, every so often, backscatter from just one or two targets in an analysis cell would be much stronger than all other backscatter. The backscatter from these targets strongly skewed the average S_V reported for the cell, causing it to no longer be representative the majority of the 5-min interval. These samples were identified and inspected, and if determined unlikely to be from individual fish or fish aggregations, they were removed from analysis with a bad data (no data) region (Figure 6).

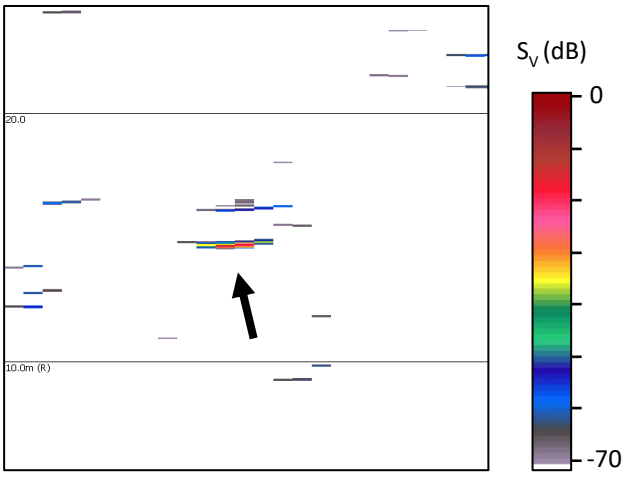

Figure 6. Example of "very strong backscatter" in stationary S_V data. This target had a target strength of -18 dB re 1 m^2, and raised the mean S_V of the 5-min sampling period by 13 dB.

Some of these strong samples appeared to be from an object moving through the beam (i.e., could be tracked across consecutive pings). Others were more difficult to identify, particularly at high current speeds, when any object moving with the current would likely only be detected in just one or two pings, and therefore could appear similar to interference from acoustic instruments.

The target strengths of these artefacts was in the area of -20 dB re 1 m^2 or more. This could be expected from marine mammals passing through the beam [34]. Large fish, such as striped bass, are another possibility, though according to the dorsal-aspect TS-length relationships found in the literature, -20 dB could correspond to a 2 m striped bass [35], whereas most striped bass tagged in the Minas Passage area have been under 1 m in length [2,9,10]. There is not much information available on the ventral TS of these organisms, but it is possible that it differs from the dorsal aspect [14].

Removing these targets meant the remaining backscatter was more representative of the majority of targets present. However, in future, other data may help determine what these targets are and if their presence is of interest (e.g. concurrent acoustic recordings of marine mammals, or detections of acoustically tagged fish by receivers).

c) *Cascading water column backscatter*. A very distinct phenomenon was visible nearly every slack tide, and was decided to be more likely related to physical processes than biological ones. This was in the form of a cloud of backscatter, often of a similar strength as fish-like targets, appearing to either rise or sink through the water column (Figure 7). This noise was in all stationary datasets but was much more prevalent during the Dec 2017-Feb 2018 dataset. It was not seen in the passes of transect 4 from the mobile dataset that were analyzed here, possibly because transects were not carried out near slack tide. The source of this backscatter is unknown but may be related to, for example, air or sediment entrained into the water column upstream of the echosounder. Data segments that were contaminated by this noise needed to be manually identified and removed using bad data (no data) regions.

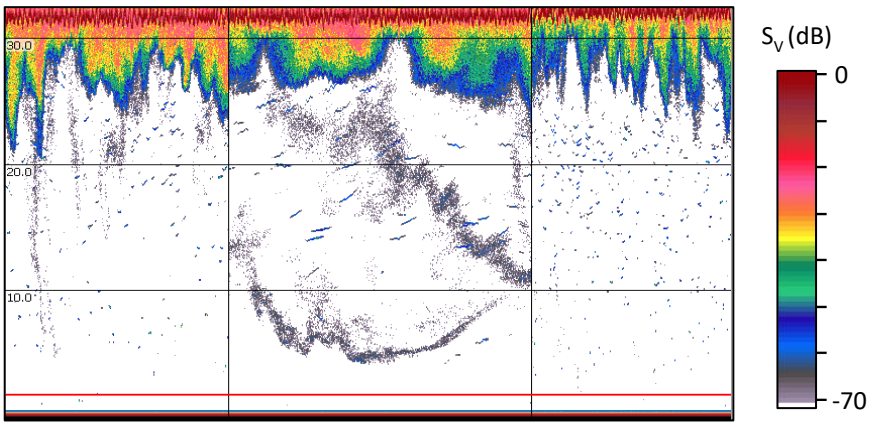

Figure 7. Example of "cascading" water column backscatter in S_V data from the stationary dataset, in this case occurring after a high slack tide.

3.3.2.3 "Transient" noise

In all stationary datasets, but not in the mobile dataset, there was a periodic increase in above-threshold backscatter spread throughout the water column (Figure 8). The source of this backscatter is unknown, though it was sometimes correlated with high current speed and/or entrained air depth. It did not appear biological in nature, given its even distribution throughout the water column. This noise tended to span two or three sequential 5-minute recording periods at each appearance. Affected cells were identified manually and omitted from the dataset.

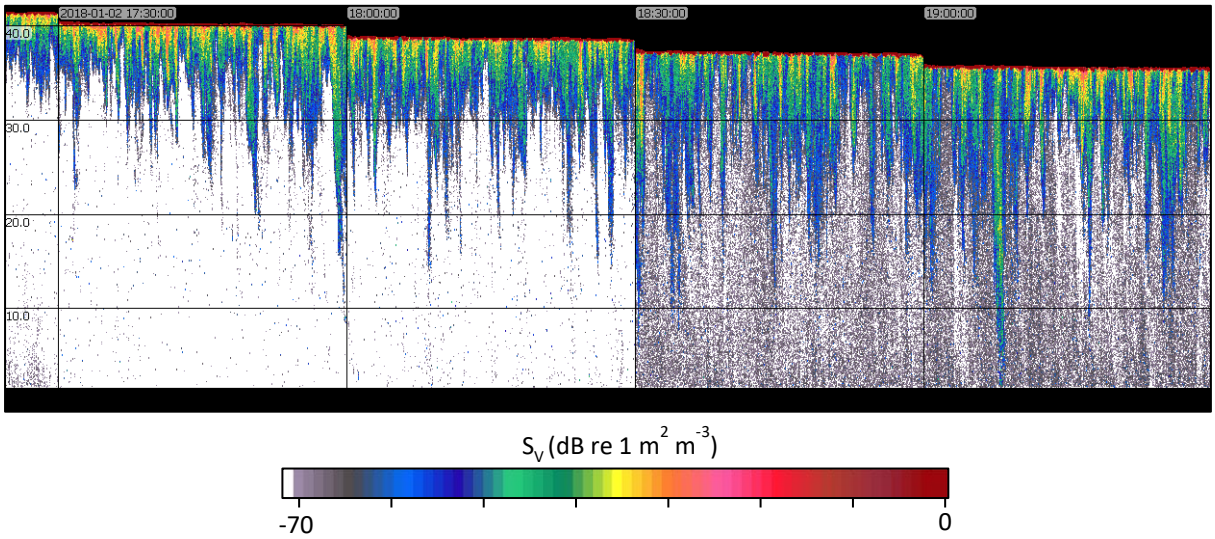

Figure 8. Example of "transient" noise in S_V data from the stationary dataset, visible in the two recording periods at the right.

Each tidal stage had a unique transient noise "profile." Slack tides were generally unaffected by transient noise. Ebb and flood tides were both more contaminated, but in different ways. During flood tides, entrained air depth and current speed were highly correlated with transient noise once current speed exceeded 2 $m \cdot s^{-1}$. During ebb tide, there was little correlation of entrained air depth or transient noise occurrence with current speed. It is possible that the interaction of current speed and direction with local bathymetry caused these differences. During ebb tide, current speed is noticeably more variable than flood tide, and direction more variable at speeds over 1 $m \cdot s^{-1}$ (Figure 9). This likely reflects the fact that many more eddies form and pass through the platform's location during the ebb tide, whereas the flow is less modified during the flood tide (see section 3.4.1 for more information on ADCP data processing).

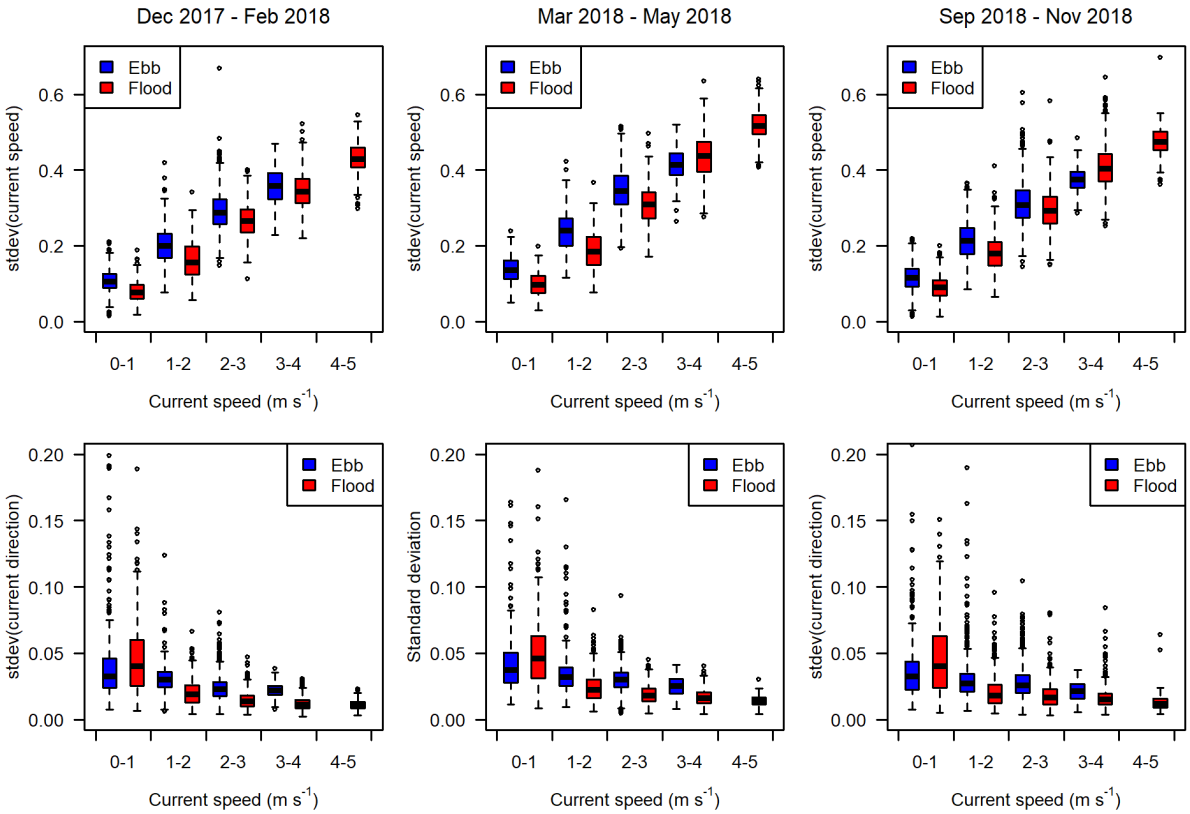

Figure 9. Standard deviation in current speed (top) and direction (bottom) for each stationary dataset, grouped by tide and speed range. Current speed and direction data were collected by the ADCP on the stationary platform and averaged for the water column. The horizontal black line is the median value, boxes span the interquartile range, whiskers extend to 1.5x the interquartile range, and points are the data falling outside of the range of the whiskers. This applies to all following boxplots.

3.3.3. Data partitioning

Once cleaned, the data were partitioned into bins with sizes chosen for the different analyses carried out, which differed by dataset.

3.3.3.1. Mobile acoustic data

Data from each pass of transect 4 were first split into equal-length distance bins that spanned the entire vertical water column. These bins measured 10 m along-track, which ensured high spatial resolution along the transect (average transect length of 1.9 km meant approximately 190 bins obtained per transect), and that every distance bin contained at least one ping (7 pings per bin on average, varying with vessel speed over ground). The echo integration results from each bin were exported from Echoview to determine the distance at which water column S_V became independent (see section 3.5.1).

The data were to then be partitioned by this distance to ensure independent samples were used in further analyses, including comparison to measurements from the stationary platform. However, it was found that water column mean S_V was already independent at the 10 m scale (details in section 3.5), so the distance bin was not adjusted.

For assessing the vertical distribution of fish, the 10-m bins were additionally partitioned into layers 1 m thick, measured upward from the sea floor.

3.3.3.2. Stationary acoustic data

Data collected from the stationary platform were partitioned first by 1-ping (1 sec) intervals, to assess at what temporal scale samples could be considered independent. This time was then used to partition each 5-minute data collection period into bins, in order to obtain a mean and variance estimate for each period.

Stationary data that were collected concurrently with each pass of transect 4 of the mobile surveys were isolated for comparisons of mean S_V and fish vertical distribution across survey methods. To assess vertical distribution, data binned by time were further partitioned into layers 1 m thick, measured upward from the sea floor.

3.3.4. Echo integration

Partitioned data were echo integrated and exported from Echoview for further analysis in R software (v3.6.2) [36]. The metric exported for use in the following analyses was mean S_V, the average volume backscatter from within the given analysis domain, in dB re 1 m^2m^{-3}.

3.4. Auxiliary data processing

3.4.1. Current speed and direction

Nortek Signature 500 ADCP data were converted from the Nortek ad2cp file format to csv format using the Nortek Signature Deployment software (v3.4.17.0). Data were exported in SDU coordinates (speed, direction, up) for further processing in R. This format provided measurements of current speed and direction (horizontal and vertical), as well as the amplitude of backscattering from the upward-facing beam of the ADCP. Average measurements were obtained for each 5-minute sampling burst. The range of the maximum amplitude from each burst was used to approximate the range of the surface, which was confirmed against acoustic data. Data in the upper 10% of the water column were then omitted from analyses to avoid any interference from side lobes (SignatureViewer v1.01.17, Nortek) (Figure 10).

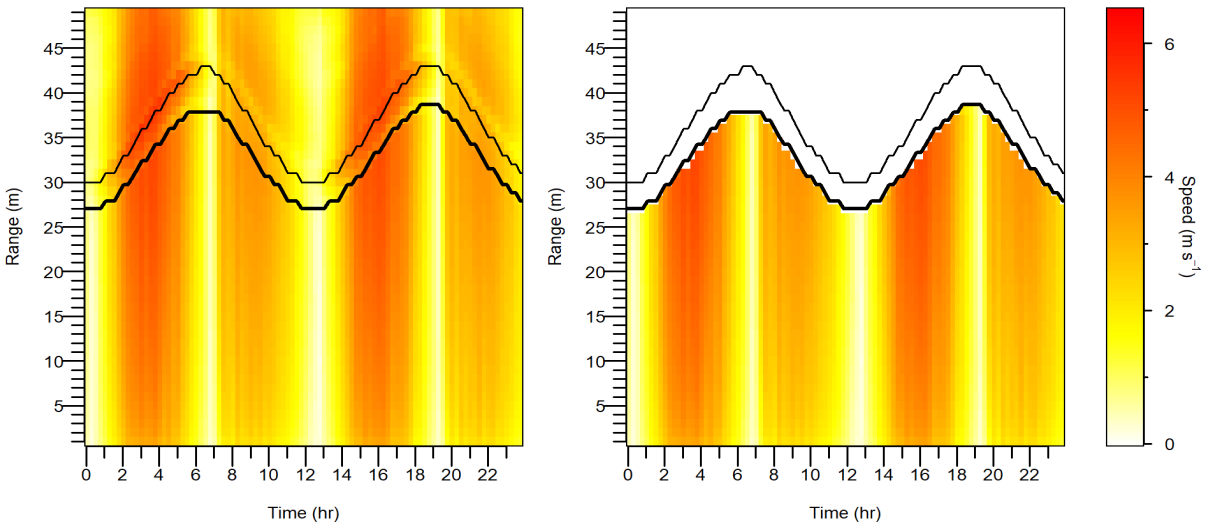

Figure 10. Example ADCP data, before and after surface backscatter removal. The thin black line is the estimated location of the surface, and the thick black line is the 10% offset from the surface.

Current direction readings were then corrected for magnetic declination (-17.22˚). Water column averages of speed and direction were obtained for each burst, and were used for defining the start and end times of each tidal stage. Slack tides were defined as periods of time when average water column current speed was less than 0.5 $m \cdot s^{-1}$. The water column average current speed and direction are summarized for each deployment in Table 3 and Figure 11. Tidal stage times determined from the FAST3 ADCP data were used for both the mobile and stationary datasets.

Table 3. Summary of water column average current speed and direction during each platform deployment.

Dataset	**Current direction (degrees)**		**Maximum current speed ($m \cdot s^{-1}$)**	
	Flood tide	**Ebb tide**	**Flood tide**	**Ebb tide**
Dec 2017 – Feb 2018	118	291	4.7	3.5
Mar 2018 – May 2018	121	295	4.5	3.4
Sep 2017 – Dec 2017	118	292	4.4	3.3

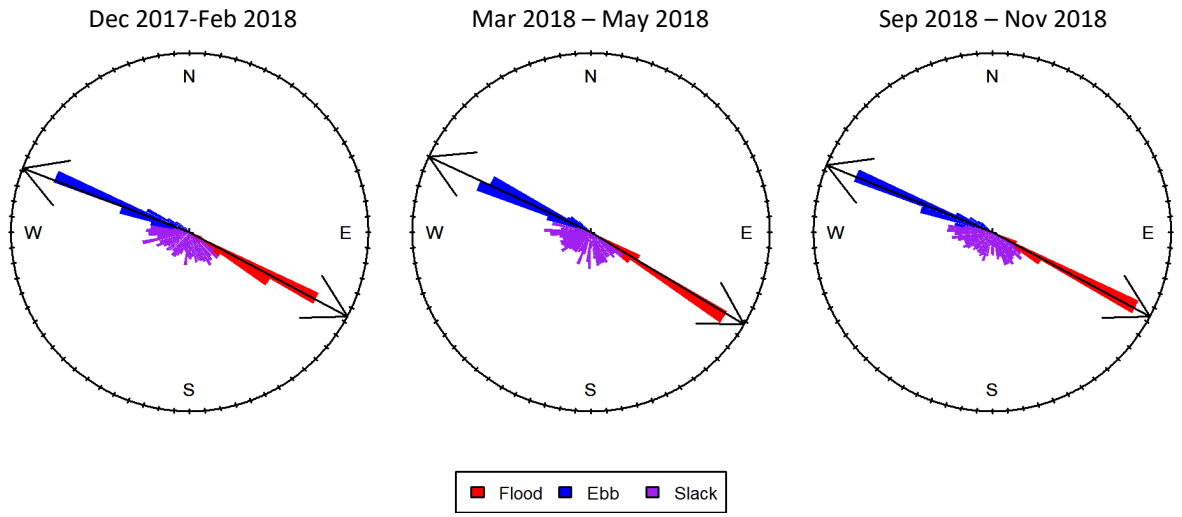

Figure 11. Average water column current direction during the three stationary platform deployments. Bar length indicates the frequency of current speed measurements within each 5-degree direction bin.

3.4.2. Salinity and temperature

Only temperature and conductivity data from the Aanderaa SeaGuard RCM were needed for the purposes of this report. Conductivity and temperature were used to calculate salinity using the code found at [37]. For the September 2018 deployment, when the SeaGuard was not functional, salinity was assumed equal to 31.5 psu, based on the range in salinity during the other two surveys, as well as salinity data from September of the previous year (note that salinity varies by approximately +/- 0.5 psu over the course of a tidal cycle).

Temperature and salinity were used to calculate the sound speed and absorption coefficient, using the equations developed by [31,32,38]. These quantities were necessary for calibrating the acoustic data (see section 3.3.1).

3.5. Data analysis

3.5.1 Spatial autocorrelation

Empirical variograms were calculated for data from each repetition of transect 4 in the mobile dataset, which were echo-integrated at 10 m resolution. Variograms plot the semivariance of points within a dataset as a function of separation distance. Semivariance is calculated as

$$\gamma(d) = \frac{1}{2n(d)} \sum_{i}^{n(d)} [(y(x_i) - y(x_i + d)]^2$$

where y is the value of the data at location x_i, and $n(d)$ is the number of pairs of data points separated by distance d [39].

Small values of the semivariance indicate strong spatial dependence, whereas larger values indicate weaker dependence. A typical variogram would be expected to have a shape similar to Figure 12, in which the semivariance increases with distance until it levels off at the "sill". After this transition point, samples are no longer spatially correlated, and the distance at which this occurs can approximate the distance to which information from a point measurement may be assumed representative [16,39]. The intercept of the variogram at 0 distance is the "nugget", which indicates the level of variation occurring at smaller spatial scales than were measured.

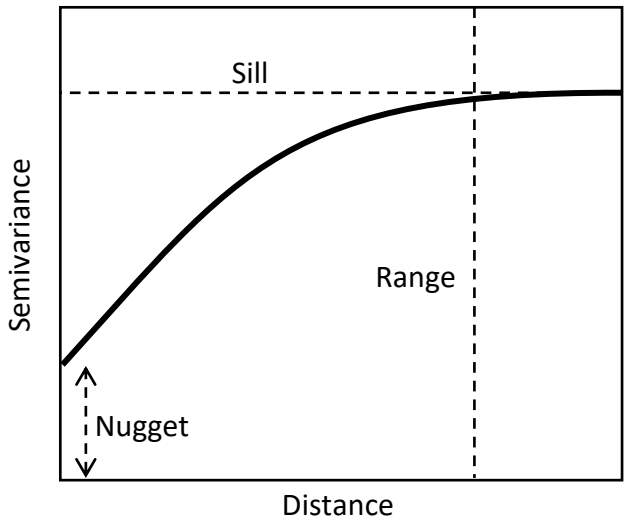

Figure 12. Theoretical shape of a variogram, showing the nugget, sill, and the distance at which samples are no longer spatially correlated.

Empirical variograms were calculated in R with the package *geoR* (v1.7-5.2.1) [40]. Null envelopes were generated for each variogram using 1000 Monte Carlo permutations. The null envelope indicates the expected variance as a function of distance, assuming spatial randomness. Points of the variogram that fall outside of this envelope indicate possible spatial dependence.

The goal was to determine the distance at which measurements became independent and to adjust the horizontal bin accordingly. However, when variograms were generated for all

transects, they were found to be nearly flat, with little evidence of the initial slope that would typically be expected (see section 4.2). This indicated a lack of spatial correlation at 10 m resolution, so bin size was kept at 10 m (but see section 4.2 for further discussion). Mean S_V measurements from these bins were assumed to be independent of each other, and were used in comparisons of mobile results to stationary.

3.5.2 Temporal autocorrelation

Temporal autocorrelation is the correlation of a time series with itself, when offset by some number of samples in time (lag). The autocorrelation coefficient, r_h, for a time series, y, at lag h, is given by

$$r_h = \frac{\sum_{t=1}^{N-h}(y_t - \bar{y})(y_{t+h} - \bar{y})}{\sum_{i=1}^{N}(y_t - \bar{y})^2}$$

where N is the number of samples in the series and $\bar{y}$ is the series' mean [41]. The autocorrelation coefficient will be 1 for a lag of 0, when the series is aligned perfectly with itself (Figure 13). Assuming time dependence in the data, a confidence band for a significance level α can be calculated as:

$$\pm z_{1-\alpha/2}\sqrt{\frac{1}{N}\left(1 + 2\sum_{i=1}^{k} r_i^2\right)}$$

where z is the quantile function of a standard normal distribution. When the autocorrelation coefficient falls within this band, samples are assumed independent.

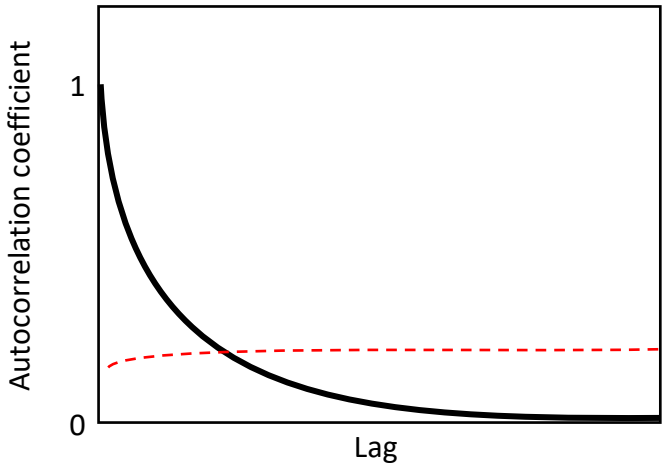

Figure 13. Theoretical shape of an autocorrelation function (ACF) of at time series, showing the 95% confidence interval.

For each of the three stationary datasets, the autocorrelation function (ACF) was calculated for every 5-minute recording period using the mean S_v values exported from Echoview in 1-ping (1 second) bins. An average ACF was calculated for each dataset, which indicated that water column mean S_V became independent at a lag of 6 seconds in each dataset (see section 4.3).

Stationary data were then partitioned into bins 6 seconds long and echo integrated. S_V mean values from these bins was used to calculate an estimate of the mean and variance for each 5-minute recording period, resulting in a new time series with half-hour resolution for each stationary dataset.

3.5.3 Comparison of mobile to stationary measurements

Stationary data collected concurrently to passes of transect 4 in the mobile surveys were identified and isolated. As stationary data were collected every half hour, measurements did not always align exactly in time, and so the nearest point in time was chosen for comparison to each mobile transect. The temporally indexed mean and variance was then compared to the mean and variance obtained for the corresponding passes of transect 4.

4. Results and Conclusions

Below are qualitative observations of the acoustic data used in this assessment, followed by a discussion of the spatial correlation of the mobile data (spatial representative range), the temporal correlation of the stationary data (temporal representative range), and the direct comparison of results from each study type.

4.1 Qualitative observations of acoustic datasets

4.1.1 Mobile data

The mobile dataset used here consisted of 36 passes of transect 4 that overlapped with stationary data collection periods. These came from 5 different mobile surveys of the FORCE test site, in Feb, Apr, May, Sep, and Oct 2018. Example echograms from each survey are shown in Figure 14. Some qualitative differences between the individual passes of transect 4 were apparent. For example, backscatter in the Feb, Apr, and May surveys consisted of mainly individual targets scattered throughout the water column. There was noticeably more backscatter in the water column during the Sep and Oct surveys. Some aggregations were visible mid-water-column in the Sep survey during the day. These differences are likely related to seasonal changes in species composition and abundance in Minas Passage [2,3,9-12].

The amount of entrained air varied by survey and was greatest in the Oct survey, which was cut short due to poor weather conditions. Most mobile data were relatively clean, but transect passes missing more than 10% of their distance bins due to contamination from entrained air or other noise were omitted from spatial analysis. This included 3 passes in the Feb survey and 1 in the May survey.

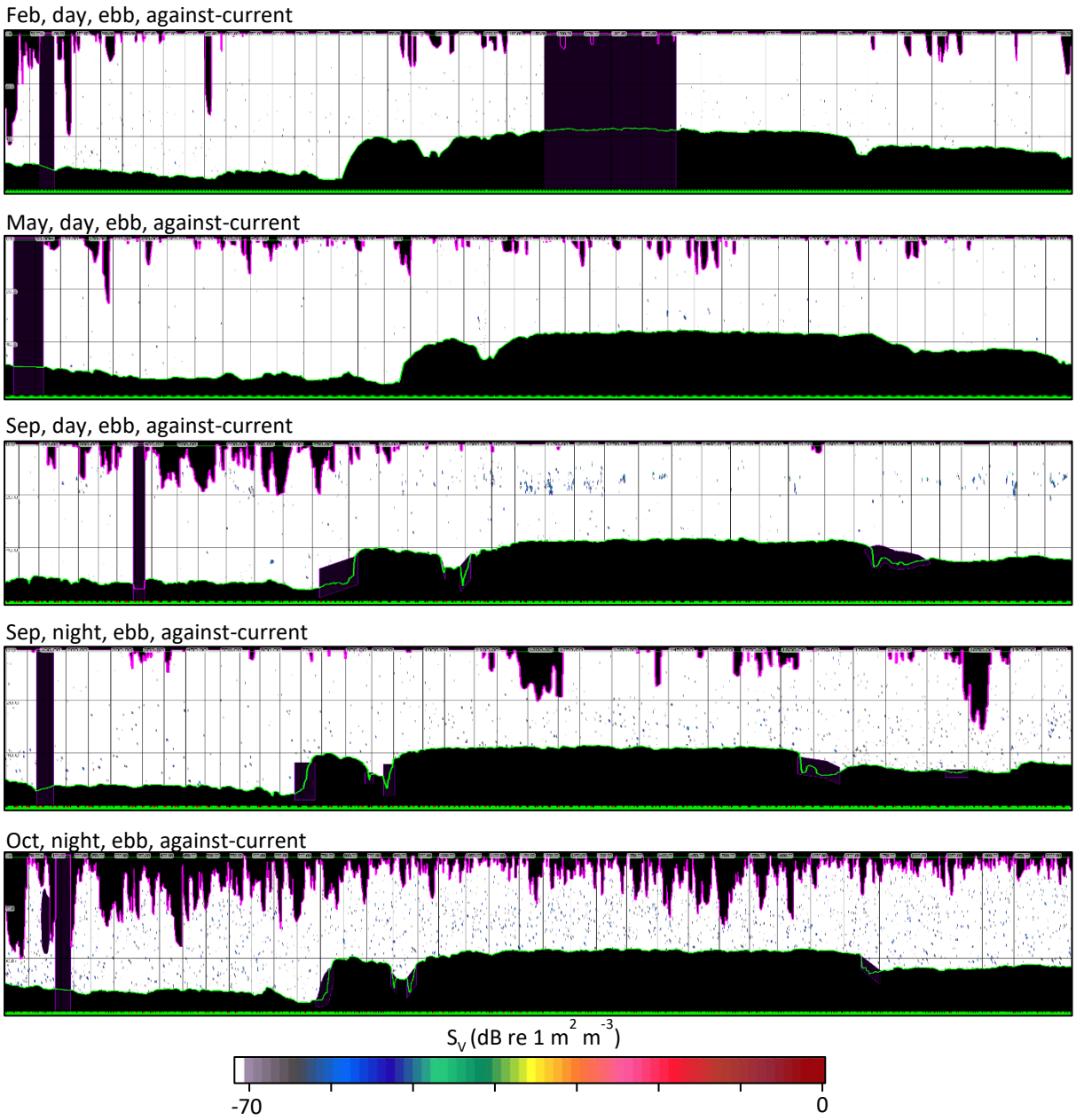

Figure 14. Example echograms from passes of Transect 4 carried out in 2018. The horizontal grid lines show depth increments of 20 m, measured from the surface downward. The vertical grid lines show distance increments of 50 m, measured along-transect. Volume backscatter (S_V) is shown, with units of dB re 1 m^2 m^{-3}. Black areas are data that were omitted (e.g., contaminated by entrained air, or below the bottom). Note that the number of targets at greater ranges will appear greater due to the beam widening with range, which is accounted for in calculations but not when viewing echograms.

Water column backscatter generally increased from Feb to Oct surveys (Figure 15). This trend is not easily seen when including the distance bins that contained empty water column. These data segments had no above-threshold backscatter in the water column, and therefore have a value of -999 dB (Figure 15a), which strongly skew the means. The trend does become apparent when the empty bins are omitted (Figure 15b). This upward trend is generally in agreement with the trends seen in the stationary dataset (section 4.1.2).

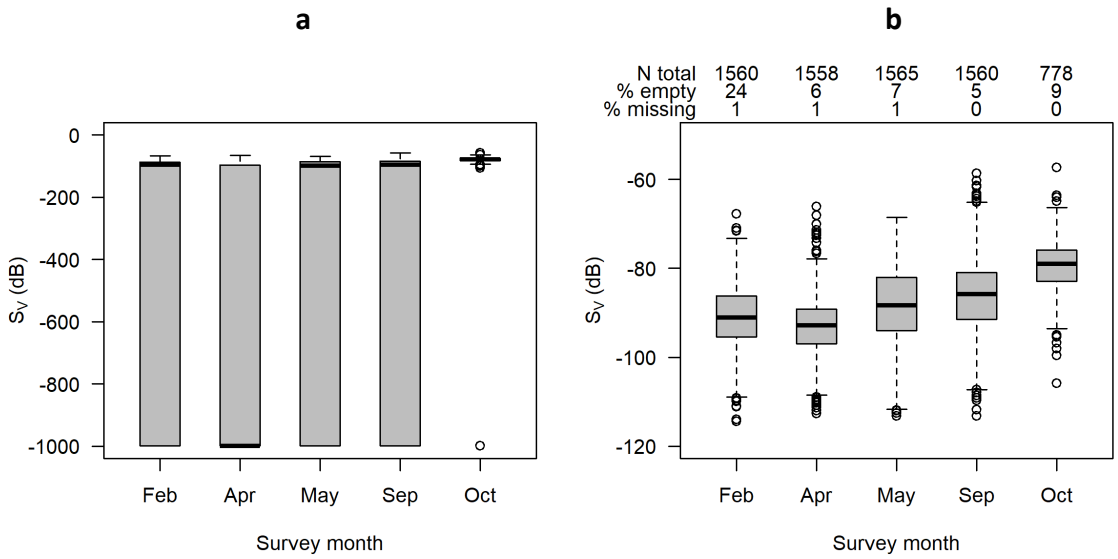

Figure 15. Summary of water column mean S_V (dB re 1 m^2 m^{-3}) from the passes of transect 4 carried out in the 2018 mobile surveys. Passes are grouped by survey month. (a) Boxplot of water column mean S_V for each survey, including the samples from empty water column (dB value of -999). (b) Boxplot of water column mean S_V for each survey, excluding empty water column samples. The total number of samples, the percent of those samples that were empty water column, and the percent that were missing due to noise contamination, are shown across the top.

Water column mean S_V was similar during the day and night in the Feb and Apr surveys, but was higher at night in the May and Sep surveys (Figure 16a). Tidal stage similarly had little effect in Feb and Apr, but in May water column mean S_V was noticeably higher during the flood tide than the ebb (Figure 16b). In Sep and Oct, ebb tide backscatter appeared slightly stronger than flood tide.

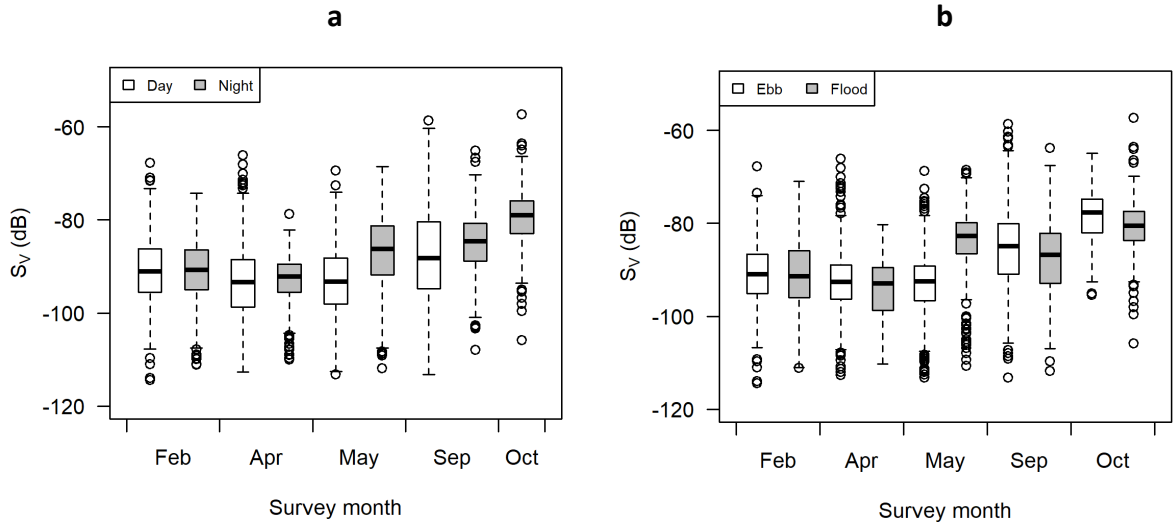

Figure 16. Summary of water column mean S_V (dB re 1 m^2 m^{-3}) from the passes of transect 4 carried out in the 2018 mobile surveys. Passes are grouped by survey month and (a) diel state (day or night) and (b) tidal stage (ebb or flood). Only results from non-empty water column are shown here.

Though surveys were spread out in time, the physical conditions experienced during each pass of transect 4 were similar, based on current speed data from the ADCP on the stationary platform. This is primarily due to the fact that mobile surveys always take place during the weakest neap tide, when weather conditions are favourable. Additionally, surveys begin after a slack tide and transects are carried out in the same order nearly every time, resulting in transect 4 sampling a similar range of current speeds across surveys. Almost all passes of transect 4 occurred in current speeds of roughly 2 to 2.5 $m \cdot s^{-1}$. The largest exception was the Feb survey, in which two passes of transect 4 occurred at lower current speeds (Figure 17). This consistency was helpful in this case, as it reduced one potential source of variance and made the passes of the transects somewhat more comparable to each other.

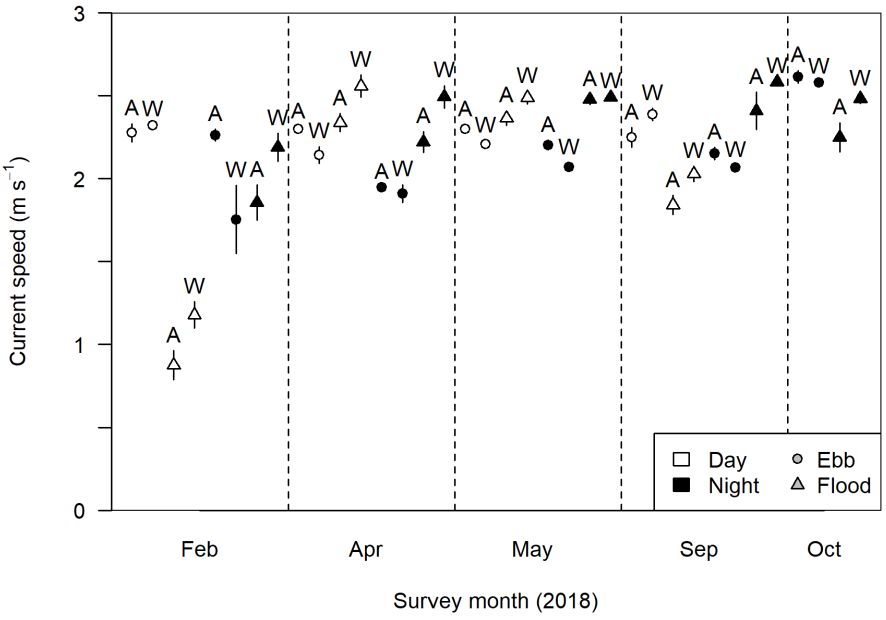

Figure 17. Current speeds during each pass of transect 4. Points are the mean current speed (+/- 1 standard deviation) during each pass, with diel and tidal stage indicated by point color and shape, and direction indicated by A (against current) or W (with current). Current speeds were obtained from the ADCP on the stationary platform.

Since the vessel would pass over the transect twice in a row, once moving with the current and once moving against, vessel ground speed differed substantially from vessel-through-water speed (Figure 18). This, too, was consistent across passes, despite the magnitude of the change in current speed that occurs with each tide. Transect passes moving with the tide essentially sampled less “water distance” than those moving against the tide, though the transects were approximately the same length over ground.

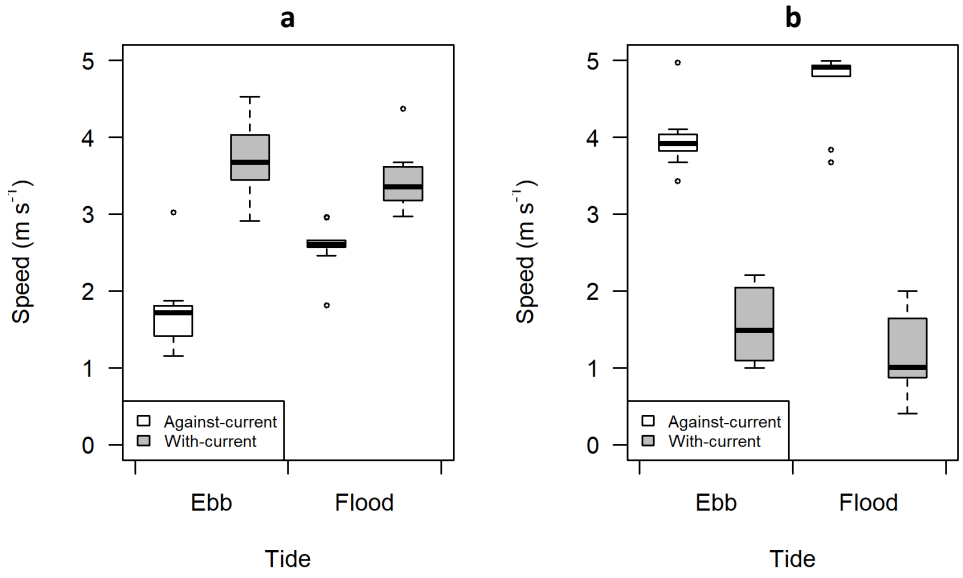

Figure 18. Vessel speed (a) over ground and (b) through water, across all passes of transect 4 in 2018, grouped by transect direction relative to flow (with or against current).

4.1.2 Stationary data

The stationary datasets spanned roughly 2 months each and captured a wide variety of backscatter from fish and other sources. Data collected from the stationary platform were noisier than data collected in the mobile surveys. This was primarily in the form of the "cascading" backscatter that appeared after slack tides, as well as the "transient noise" that would often appear at higher current speeds. Much of this noise may have simply been avoided by the mobile surveys because they occurred on the neap tides, when transient noise was rare, and during the flowing tide, when the "cascading" backscatter would not usually occur.

Another possible reason for higher noise levels in the stationary data is the pulse duration used by the echosounder. The pulse duration was shorter for the stationary echosounder than the mobile one, which increases its bandwidth and therefore potentially opens it to a broader range of unwanted backscatter [14]. The pulse duration was chosen after a test deployment which cycled through a range of operation settings; however, that deployment was closer to shore and may not have sampled the same range of conditions as the longer-term deployments mid-passage. Whether this contributes to noise in the stationary dataset could be determined with another deployment at this site, during which the echosounder cycles repeatedly through pulse length settings.

The Dec 2017 – Feb 2018 dataset had the highest levels of contamination due to entrained air, cascading backscatter, and transient noise. 57% of the recording periods were omitted, as opposed to 39% and 37% for the Mar and Sep datasets, respectively. This was potentially related to winter weather. Stronger winds were recorded during the collection of the Dec dataset than the other two (FORCE weather station data, accessible at www.oceannetworks.ca), which could have increased the amount of air entrained into the upper water column and subsequently drawn down by turbulence.

Biological backscatter was visibly different across the stationary datasets. The Dec-Feb dataset was characterized by individual targets spread throughout the water column, without much noticeable change across tides or between day and night (Figure 19). There were occasional bubbles rising from fish, possibly indicating the presence of Atlantic herring (these have been known to release swim bladder gas through the anal duct) [42].

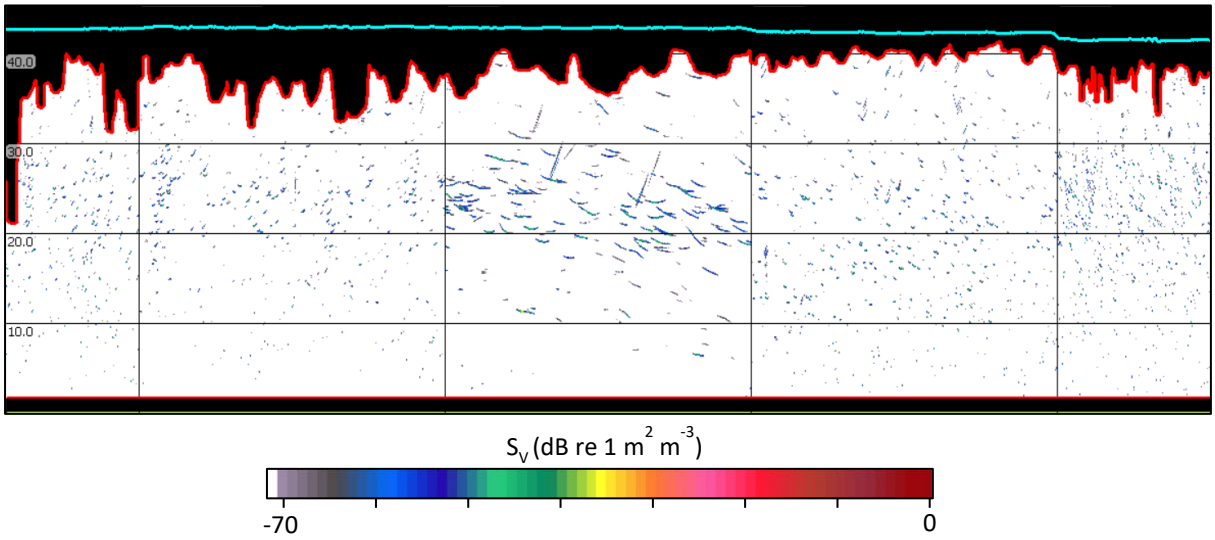

Figure 19. Example volume backscatter (S_V) data from the Dec 2017-Feb 2018 stationary, up-looking dataset, showing individual targets spread throughout the water column. In this example, slack tide occurred in the center recording period, where fish tracks are most evident and the straight angled lines potentially indicate bubbles released by fish. Vertical gridlines are the edges of each 5-minute recording period, occurring every half hour. Horizontal gridlines indicate range, measured upward from the transducer (10 m increments). Black areas are data that were omitted; e.g., contaminated by entrained air (upper red line), within the nearfield (lower red line), or above the surface (cyan line).

Backscatter in the Mar-May 2018 dataset changed noticeably from the start to the end, from more evenly-distributed individual targets at the beginning to a mix of very numerous individual targets and small, dense aggregations toward the end, with aggregations more common during the day than the night (Figure 20).

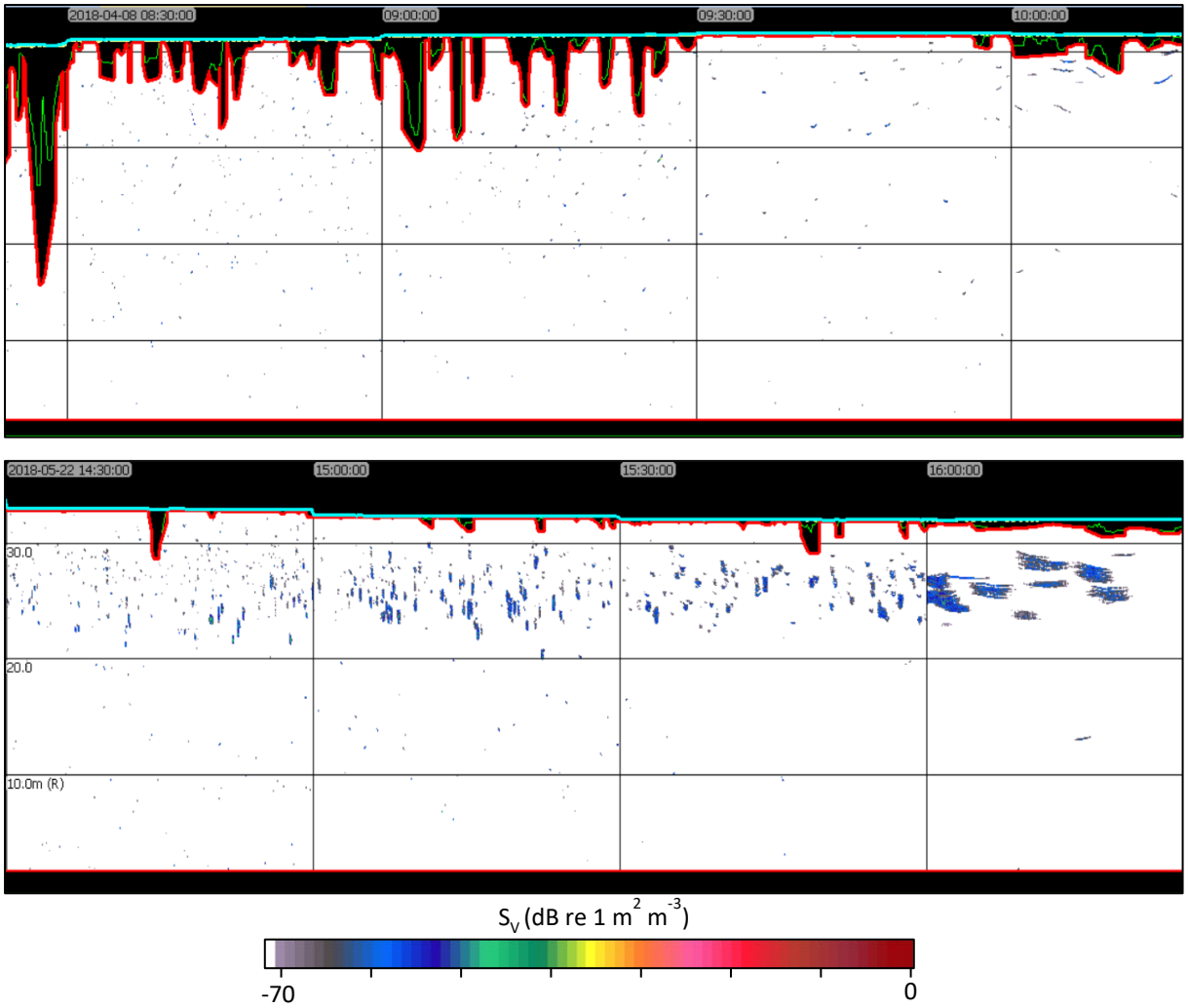

Figure 20. Example volume backscatter (S_V) data from the Mar-May 2018 stationary, up-looking dataset. Top: early April backscatter, showing individual, spread out targets. Bottom: late May volume backscatter, showing small aggregations appearing as the tide approaches low slack. Times shown are in UTC.

The Sep-Nov 2018 dataset was characterized by numerous individual targets throughout the water column, as well as numerous aggregations in the upper water column (Figure 21). These were more prevalent during the day than at night.

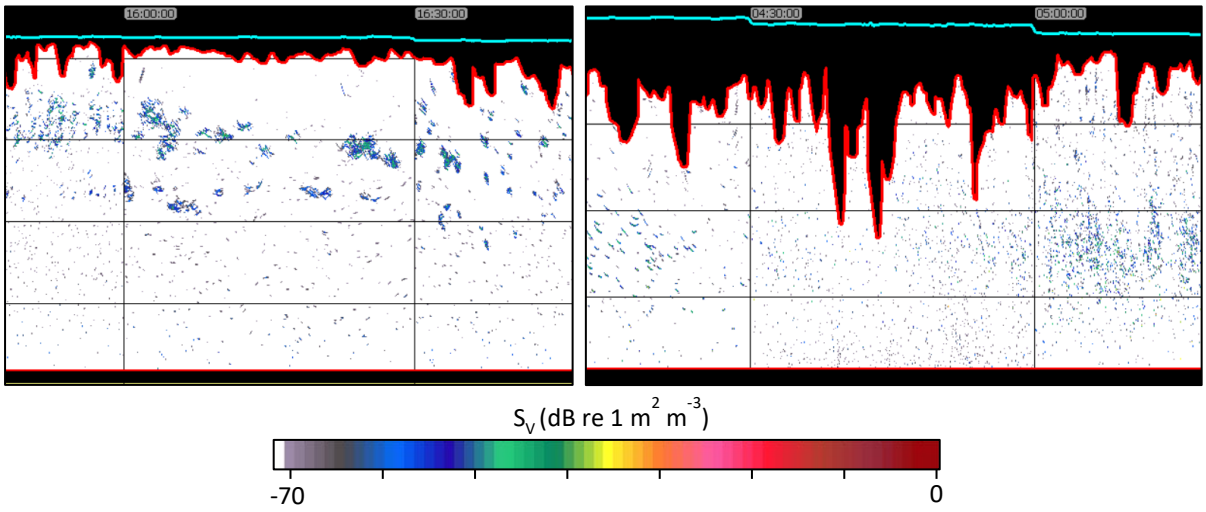

Figure 21. Example volume backscatter (S_V) data from the Sep-Nov 2018 stationary, up-looking dataset. Left: daytime example from Sep 24, showing aggregations in the upper water column and individual targets spread throughout. Right: night example from the same day, showing targets spread throughout the water column. Times are in UTC.

The changes in how fish were distributed in the water column (e.g., spread out vs. in aggregations) throughout the year are likely related to the species present, and how they are using the passage. For example, Atlantic herring are a schooling species and are present in the passage for most of the year [2,3,10,11]. However, aggregations of fish were only seen in data from the spring through fall months. This may be the result of differing behaviour based on environmental conditions, e.g. temperature, which has been found to affect the behaviour of striped bass in the passage [2]. Of course, there are other schooling species present in the passage depending on the time of year, and the presence of aggregations in the data is likely to also be related to their seasonal presence [2,3,10,11].

Overall, water column backscatter decreased from Dec 2017 through Feb 2018, increased from Apr to May 2018, and remained relatively constant from Sep to Oct 2018 (Figure 22). This trend is generally in agreement with the mobile surveys, which each sampled a much shorter period of time each. As for the mobile data, these changes in backscatter likely reflect shifts in fish abundance and community composition. Also, in both mobile and stationary datasets, variability in water column backscatter was generally larger than the change in the average from one month to the next.

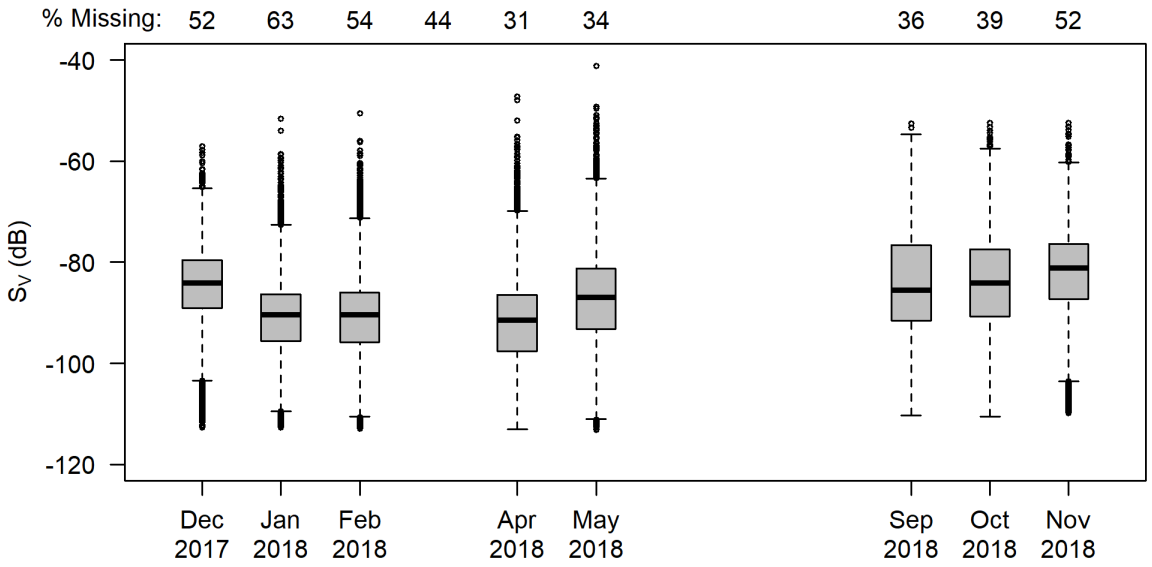

Figure 22. Water column S_V (dB re 1 m^2m^{-3}) for each month of data collected from the stationary platform. Each data point represents the water column mean for a 6-second time bin. The percentage of bins that were missing from each group due to noise contamination is shown at the top.

Diel differences in water column backscatter came and went throughout the three stationary datasets (Figure 23). Water column backscatter was higher during the night in December 2017, then the same during day and night until mid-April, when once again backscatter became higher at night through Nov 2018. This is likely a biological signature, as many fish change their behaviour diurnally [2,43-46]. The echograms show that this difference arises from noticeably more targets spread throughout the water column at night than during the day (e.g., Figure 21). These data cannot tell us where these fish go during the day, just that they are, apparently, not within the sampled volume at that time. The lowermost 2 m of water column, the uppermost portion (masked by entrained air), and anywhere else in the cross-section of the passage are all possibilities.

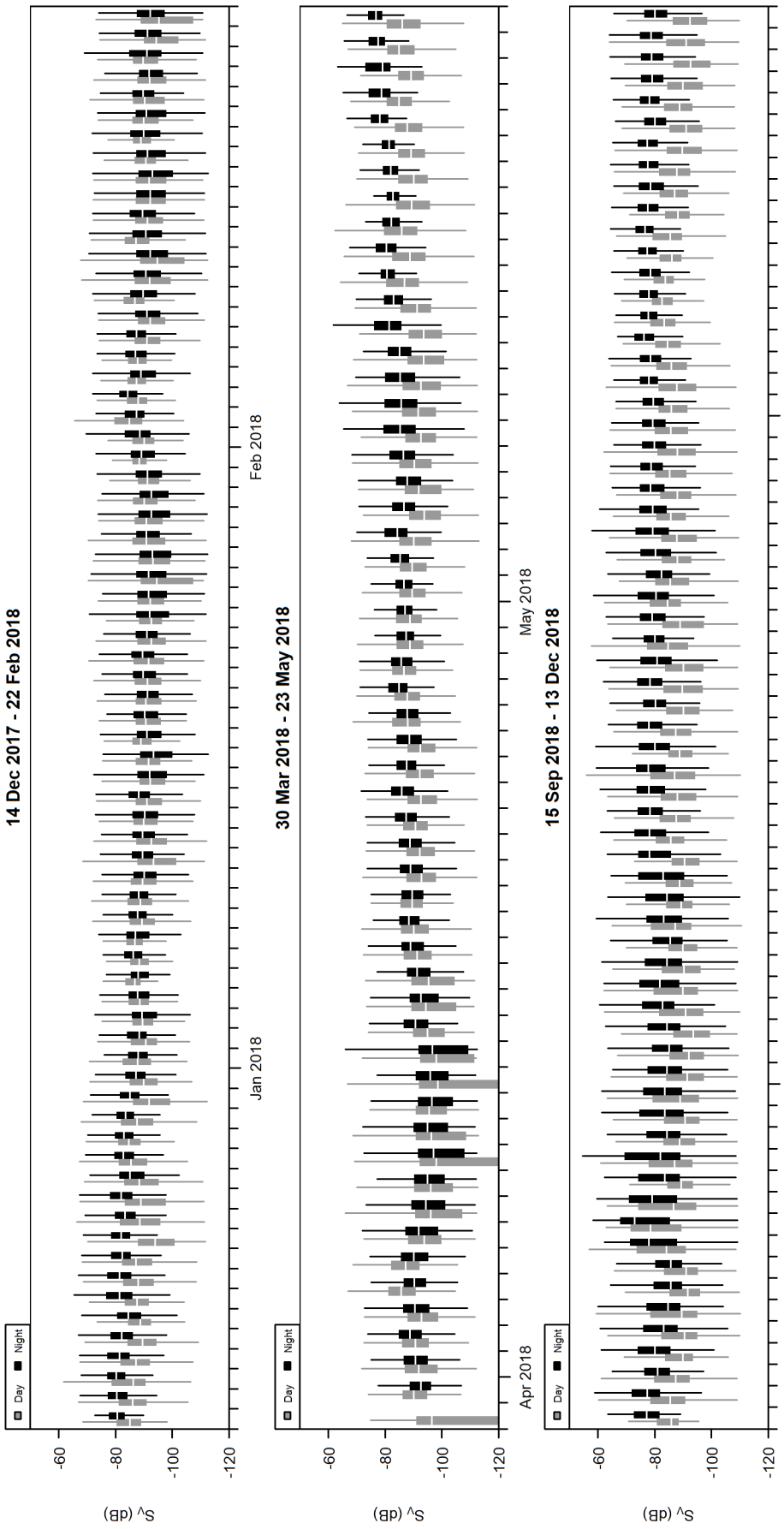

Figure 23. Water column mean volume backscatter (S_V, in dB re 1 m^2m^{-3}) for the three stationary, up-looking datasets, grouped by date and diel stage (day or night).

When volume backscatter data were grouped by tidal stage, there was not as clear a pattern as for diel stage. However, across months, low tide had consistently lower and more variable backscatter than other tidal stages, and more instances of empty water column (Figure 24).

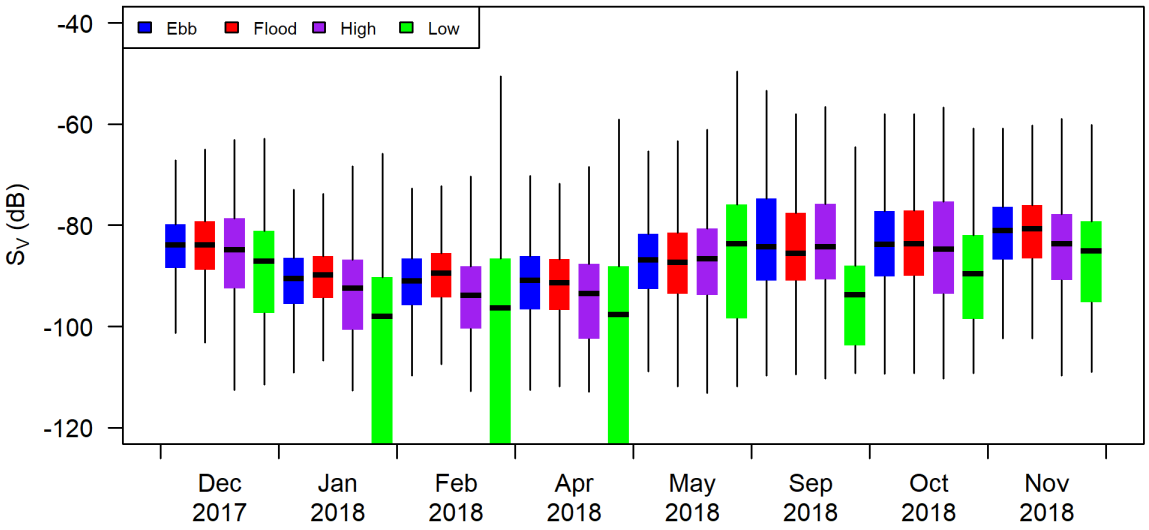

Figure 24. Water column mean volume backscatter (S_V, in dB re 1 m^2m^{-3}) for each month of data collected from the stationary platform, split by tidal stage. Boxes that extend beyond the lower limit of the plot are due to high prevalence of bins containing empty water column (S_V = -999 dB).

4.2 Spatial autocorrelation

Spatial autocorrelation was not evident in backscatter from the passes of transect 4, regardless of survey month, transect direction (with or against the current), tidal stage, or diel stage. This was clear in the empirical variograms for each pass (Figure 25), which showed almost no slope or indication of a transition point between nugget and sill. For most passes of transect 4, nearly all variogram points fell within the null envelope, indicating low likelihood of spatial dependence in water column backscatter measured along the transect.

A few passes had one or two points that fell outside of the null envelope at shorter distances, and a shape closer to what would be expected in a typical variogram (e.g., the third variogram for the Sep survey, Figure 25). This could potentially indicate some level of spatial dependency (up to 70-220 m) during these passes. However, this was not clear or consistent across transect passes, and isn't enough to draw conclusions about representative range.

The lack of correlation at the along-transect resolution tested (10 m) could occur under a few scenarios. First, the data could in fact be spatially correlated, but at a scale smaller than the 10 m resolution we were able to use. In this case, all samples would have been from the "sill" portion of the variogram, and the resolution would not have been fine enough to characterize the start of the sill. Second, the backscatter could have been spatially correlated at a scale larger than we were able to sample—that is, at distances greater than

the length of the transect. A third possibility is that both our sampling resolution and range were sufficient, and backscatter simply has no spatial structure at this site under the conditions sampled.

The echograms from the mobile surveys show an almost uniform distribution of targets along each pass of transect 4. Any spatial structure within a transect would therefore occur at quite a small scale, if present at all, and while there are no larger-scale changes obvious to the eye in the echograms (e.g. at 10's of m), it is not impossible that these could emerge if a larger distance were sampled. At the scale of our observations, the echograms and the variograms together suggest a lack of spatial correlation in the backscatter measurements made along transect 4.

Though the amount of backscatter in the water column changed over the course of the year, in accordance with the seasonally changing fish community of Minas Passage, the spatial distribution of the backscatter throughout the water column was relatively consistent in the mobile survey echograms. This is interesting, because one might expect the behaviours of different species and life stages of fish to be reflected in the echograms. Some changes were seen—for example, there were some loose aggregations visible in the daytime Sep passes of transect 4. This roughly agrees with stationary data, which show an increased presence of aggregations in May, Sep, and early Oct relative to the winter months. However, the stationary data also revealed that aggregations were most common near slack tide. During the running tide, targets appeared more dispersed throughout the water column (Figure 20). Mobile surveys all took place during the running tide, which may explain why they did not show much difference in fish distribution in the water column over time. This may also indicate that aggregation is influenced by the current speed. For example, aggregating fish species may not be forming aggregations at high current speeds, or are outside of our sampled volume (e.g., within the entrained air layer).

The apparent lack of spatial structure here contrasts with results in [16] from Puget Sound, where there was significant correlation along transects to a distance of 300+ m. Transects in that study were conducted across-current, whereas transects in this study were conducted parallel to the current. It was expected that fish biomass would show stronger correlation over distance when moving parallel to the flow than perpendicular, as the water moving through the echosounder is the same moving mass. Instead, no spatial correlation was observed in our transects at the resolution we sampled. This site is also very different from the Puget Sound site in [16]. Current speeds in Minas Passage are stronger, and mixing potentially more intense, than the Puget Sound study site, and it is possible this simply disrupts any attempt at spatial coordination by fish, at least at the scales observed here.

Given the apparent lack of spatial structure in water column backscatter at the scales observed, it is difficult to say whether data from the stationary platform (located 40 m away from the nearest point of transect 4) are directly comparable, even when collected concurrently.

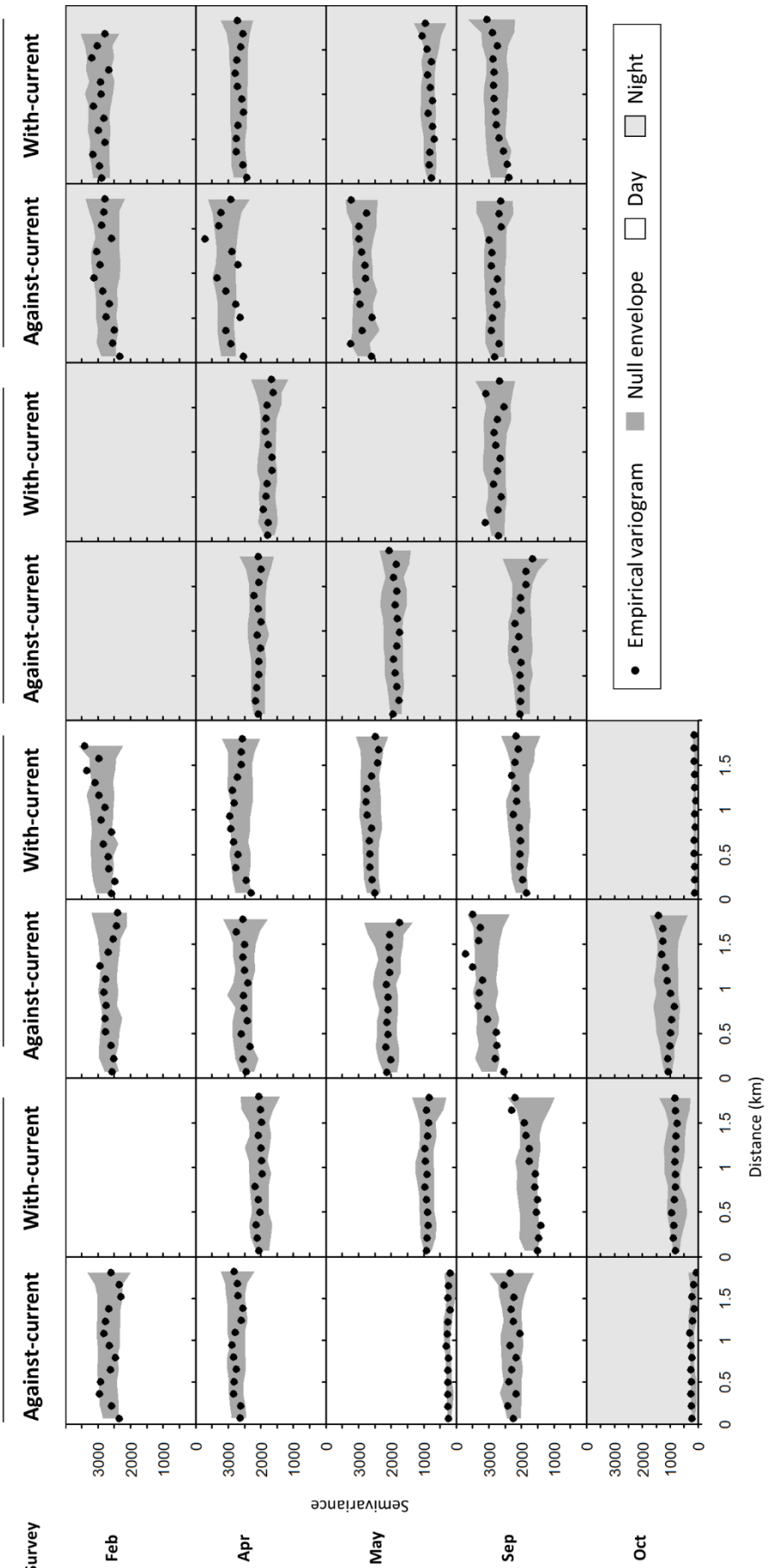

Figure 25. Variograms for repeated passes of transect 4, for mobile surveys conducted in 2018. Points are the empirical variogram, and the dark gray shaded region is the null envelope. Blank plots occur if too much of the transect was contaminated by noise to be used. Light gray backgrounds indicate data collected at night.

Analysis of data collected from all transects across the survey area, including examination of correlation with- and across- the direction of flow, would provide further insight for interpreting these results. In this example, the current regime was similar across most transect passes (Figure 17), making the individual passes more comparable to each other. When incorporating information from the other transects, which occur at different but consistent points in the tidal cycle, it will be important to account for the differing current regimes sampled by each, as this is likely to affect fish presence and distribution.

4.3 Temporal autocorrelation

Water column mean S_V measurements made from the stationary platform were found to become independent at 6 seconds for slack tide periods and at 3 seconds in ebb or flood tide periods, in all three stationary datasets (Figure 26). This makes sense, given more water passes by the transducer between pings at higher current speeds than at lower ones.

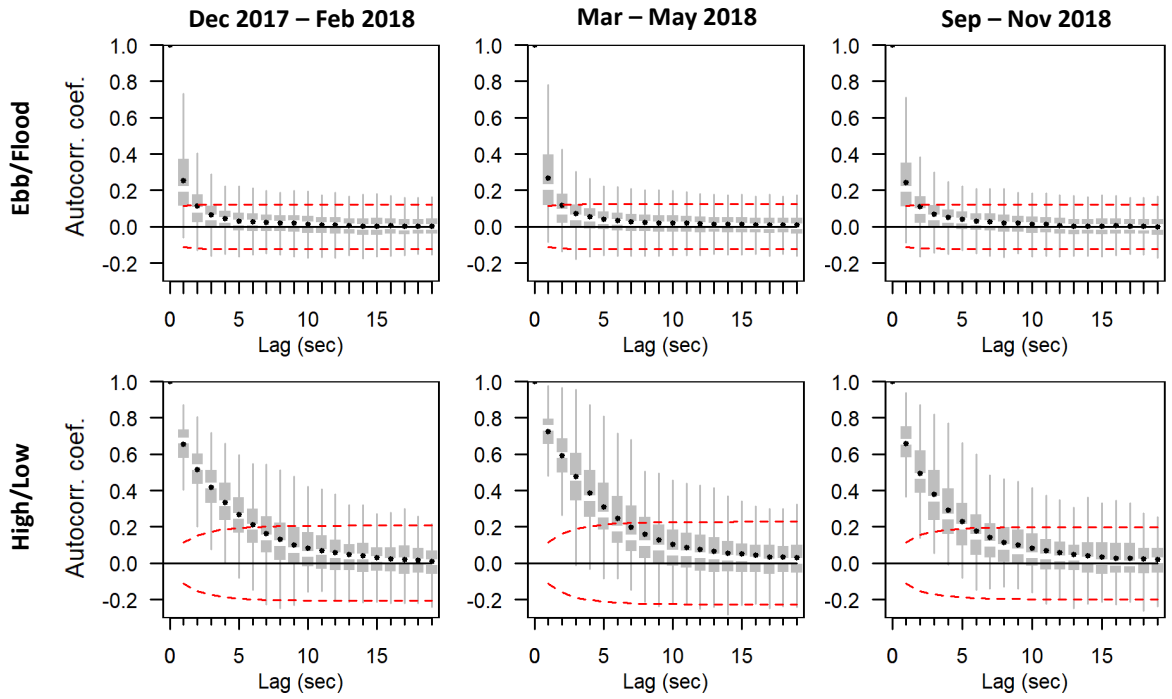

Figure 26. Autocorrelation function (ACF) for each stationary dataset at 1-second resolution. Top: running tides (ebb or flood); bottom: slack tides (high or low). The gray box plots show the distribution of the autocorrelation coefficients from each recording period, the black points indicate the average across all recording periods, and the red dashed lines are the 95% confidence interval.

Platform S_v data were subsequently binned at 6 second resolution to acquire a mean and standard deviation for each 5-minute recording period, occurring each half hour. The resulting half-hour resolution time series showed large amounts of variability on short time scales (hours), primarily related to tidal and diel periodicities in water column backscatter. This was clear in the ACF for each dataset's half-hour time series (Figure 27), with spikes in correlation aligning with 6.2, 12.4, and 24 hour lags, and at times significant correlation near larger tidal harmonics, including 13.7 and 27.6 days (particularly in the Sep-Nov 2018 data). When a 24-hour moving average was used to remove the shorter-scale variation, these peaks were removed, revealing that the underlying trend (unrelated to tidal or diel cycles)

remained autocorrelated up to approximately 3 days. The same pattern was found regardless of whether empty bins were kept in the dataset or not, and for variance estimates as well.

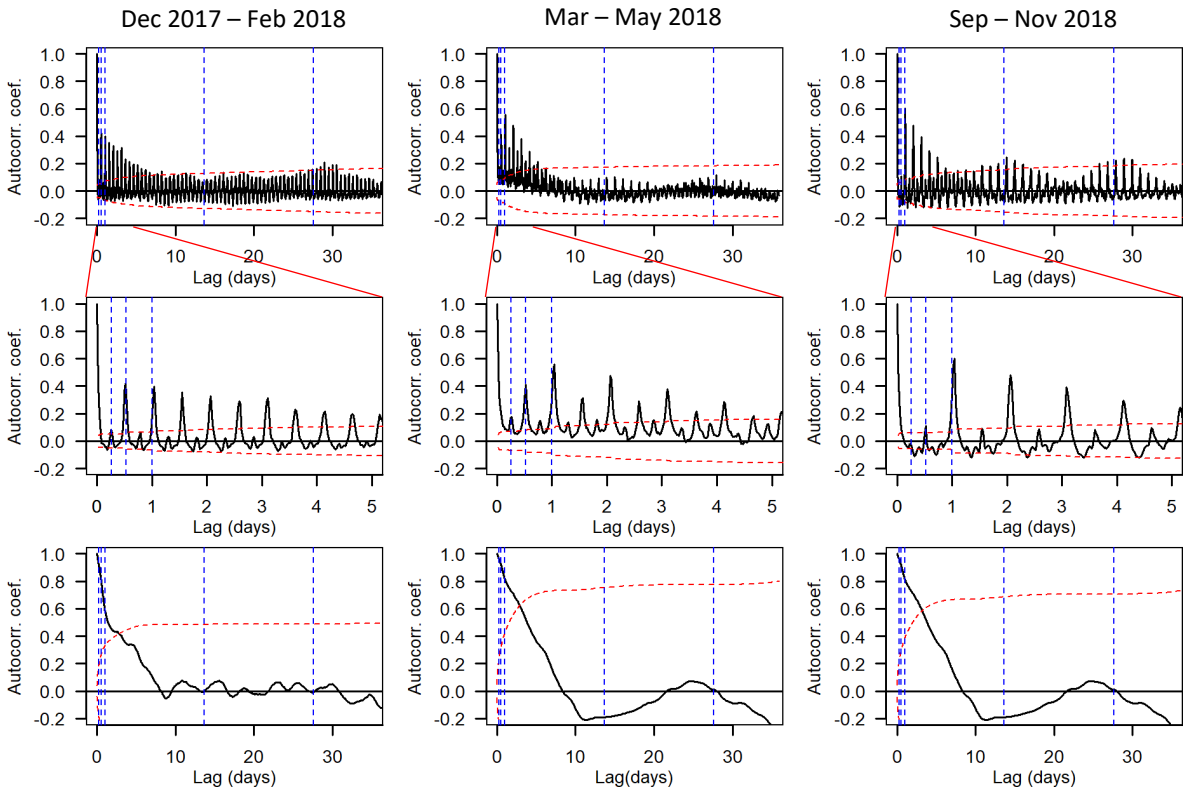

Figure 27. Autocorrelation function (ACF) for each half-hour time series of mean water column S_V generated from the stationary datasets. The black line is the autocorrelation coefficient, the red dashed line is the 95% confidence interval, and the blue vertical lines indicate relevant tidal and diel periodicities (6.2, 12.4, and 24 hrs, and 13.7 and 27.6 days). The top row shows the entire ACF, the middle row zooms in on the smaller lags, and the bottom row shows the ACF of the time series after a 24-hr rolling average filter was applied.

The cyclic variation introduced over the course of a tidal cycle or a day was often greater than the magnitude of the trend observed over the duration of the dataset. This was particularly true if bins that sampled empty water column were included when calculating the time series. For the sake of visualization, these empty points were removed, and the scale of the short-term variation can be more easily compared to the scale of the long-term changes (Figure 28).

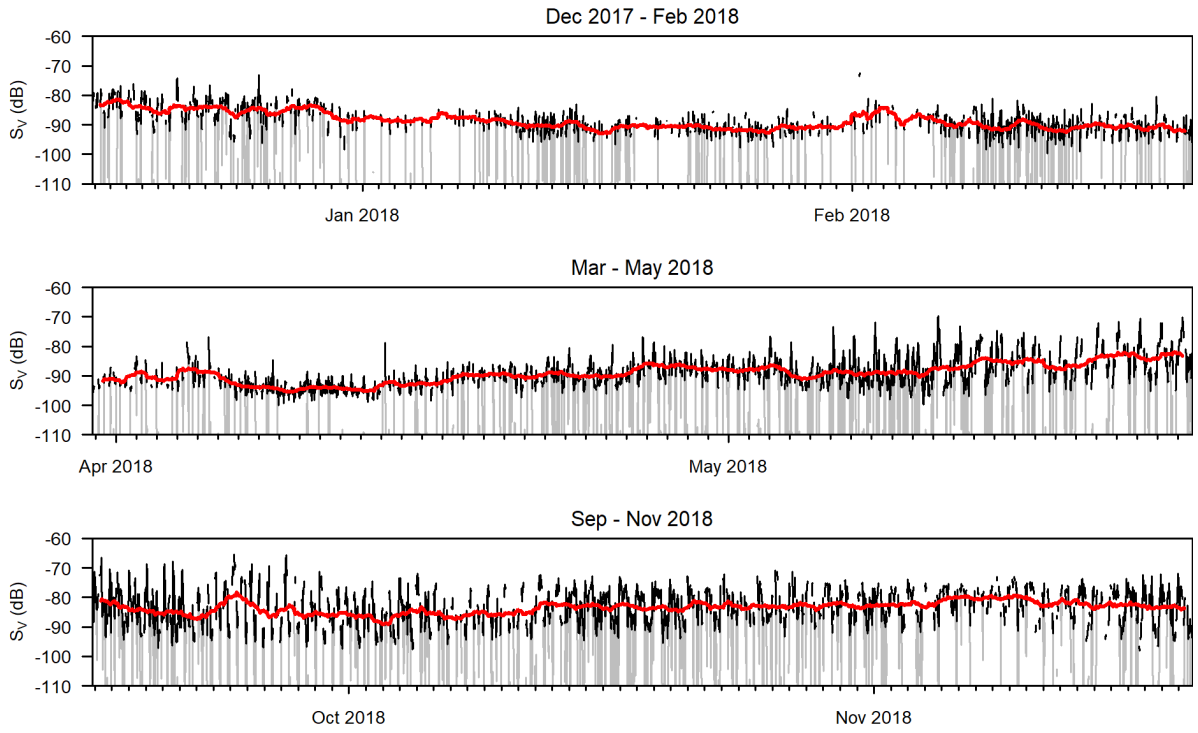

Figure 28. Water column mean S_V from stationary data, calculated for each recording period (5 minutes every half hour). Gaps exist where bins were missing more than half of their samples due to noise contamination. The gray line is the mean when empty water column bins are included in the calculation. The black line is the mean calculated without empty water, and the thick red line is the rolling mean calculated with a 24 hour window (excluding empty water).

Removing the empty water column values helps with data visualization; however, the absence of fish (the presence of empty water column) is important information that should not be eliminated from analyses. The ACF for the number of empty samples per recording period showed the same clear tidal and diel variation as the mean water column Sv (Figure 29), indicating fish presence/absence, in addition to density, is linked to these cycles.

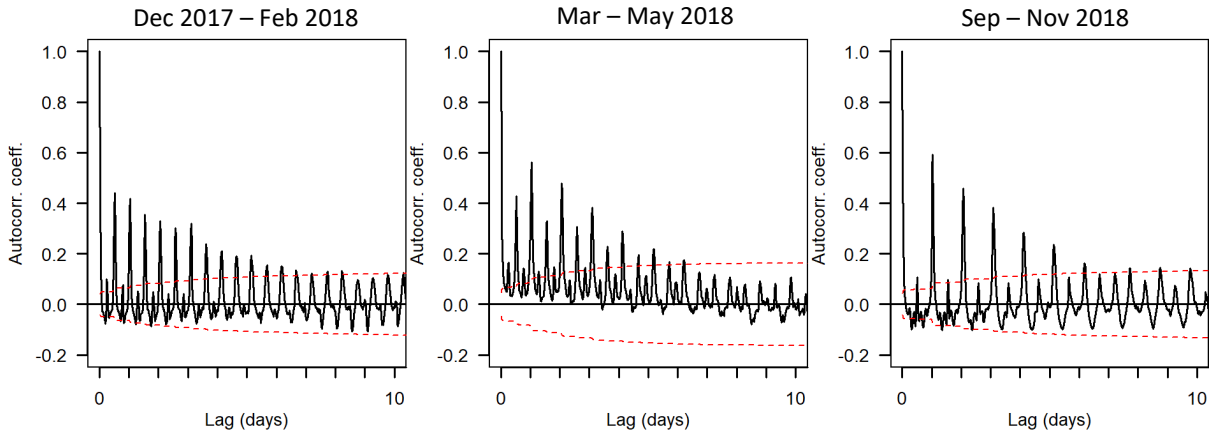

Figure 29. Autocorrelation functions for the number of empty bins per sampling period, for each of the stationary datasets.

Understanding when there are no fish present in the water column would be useful for assessing potential effects of tidal power devices. This would require a better quantitative approach for handling zero-values. One option to explore would be a two-stage model of backscatter, e.g. a delta model, which first models the probability of zero occurrence, then non-zero values [47].

The large degree of variation in fish presence and backscatter strength related to tidal and diel cycles reinforces the importance of samples spanning at least one day when seeking to monitor long-term trends with short, discrete surveys. Twenty-four hours of data allow quantification of the scale of this variation, and computation of a mean that can aid in long-term monitoring. The three stationary datasets examined here indicated that a 24 hour average may have a representative range of up to 3 days.

4.4 Comparison of mobile to stationary measurements

Direct comparison of water column mean S_V across the mobile and stationary datasets revealed differences in the results from each survey type. When just the nearest 5-minute stationary period was compared to each pass of transect 4, results were grouped but not highly correlated (Figure 30). Including empty water column segments (-999 dB) in the calculation of the mean and standard deviation for each transect (mobile data) or recording period (stationary data) strongly skewed the means toward large negative values, particularly for mobile transects, which had more empty water column segments (Figure 30a). If empty water column segments were omitted from each survey type, there was better agreement across them (Figure 30b). However, there was still a good amount of variation between the two, which appeared to be independent of tidal stage or whether the mobile transect was moving with or against the current. A linear model fit could only explain 23% of this variance ($S_{V\_stationary}$ = - 22.0 + 0.75*S_{V_mobile}).

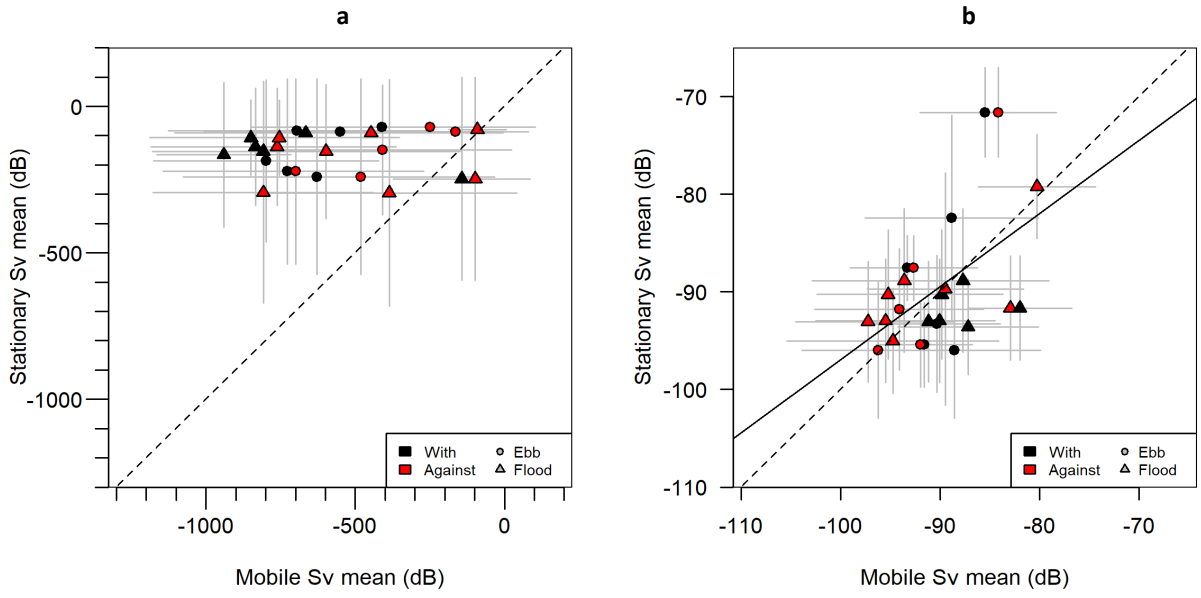

Figure 30. Average (+/- 1 standard deviation) water column mean S_V for stationary data vs mobile data, comparing each pass of transect 4 to the nearest 5-min stationary collection period, (a) including empty water column samples, (b) excluding empty water column samples. The dashed line is the 1:1 line, and the solid line is the linear fit.

Though the results from each survey type did not agree well when each transect pass was directly compared to the closest 5-min period from the stationary data, when data were instead grouped by day, the results agreed much more closely (Figure 31). When the empty water column bins were removed (Figure 31b), the agreement between the two was almost 1:1 ($S_{V\_stationary}$ = - 8.8 + 0.90*S_{V_mobile}, adjusted R-squared = 0.94).

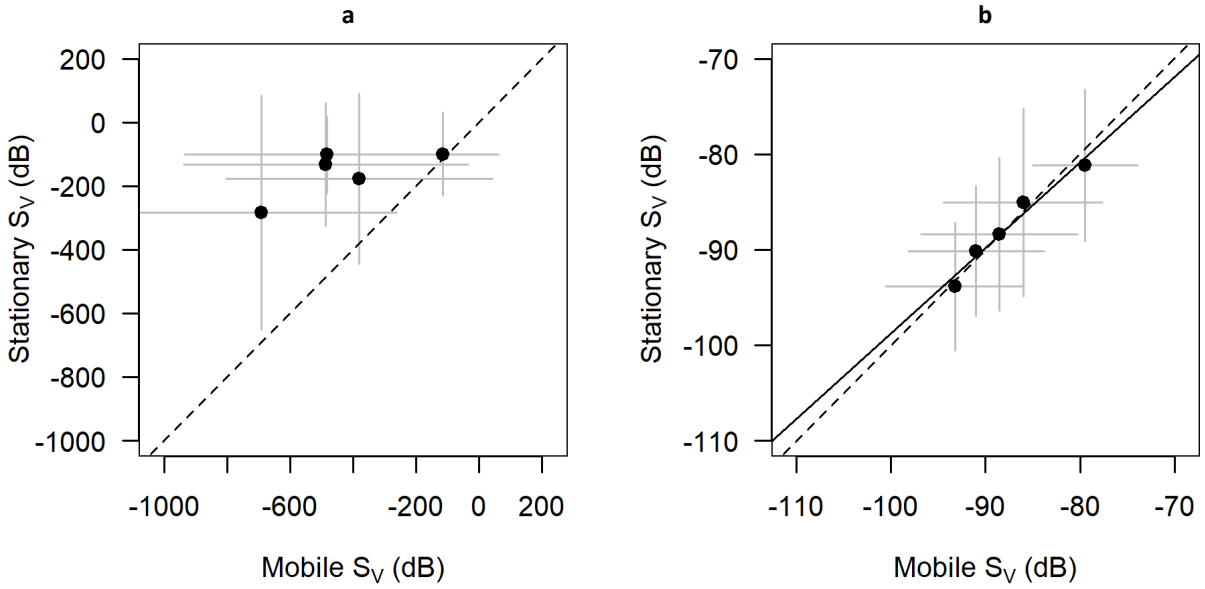

Figure 31. Average (+/- 1 standard deviation) water column mean S_V for stationary data vs mobile data, grouping mobile surveys by day and comparing to the corresponding 24 hours of stationary data, (a) including empty water column samples, (b) excluding empty water column samples. The dashed line is the 1:1 line, and the solid line is the linear fit.

Agreement at the scale of one day, but not at a scale of minutes, makes sense given the temporal variability described by the stationary dataset. Backscatter at this site changes drastically over shorter time scales, but a 24 hr average can provide more reliable data points for quantifying longer term trends.

Given that the two survey types agreed well when the 24 hr average was compared, it is possible that spatial variation at this scale (the platform was 40 m away from transect 4) was negligible in comparison to the temporal variability.

The vertical distributions were not, in the end, compared across sampling types, as there was simply not enough non-empty 1-m vertical bins to create a useful comparison. There is the additional issue of varying amounts of water column being sampled at any given moment due to entrained air, whether mobile or stationary, which complicates comparison of fish vertical distribution across any separation in time or space. Given that half of the water column is often missing, vertical distributions may not provide particularly useful information at this site, at least during the running tide. Proportions of fish at each layer would not be meaningful if the proportion of the water column sampled is constantly changing. One approach may be to manually isolate very clean segments of data specifically for the purpose of analysing the vertical distribution of fish. However, extrapolation of

results beyond these time periods (e.g. to times of faster speeds or rougher weather) could be difficult to justify.

5. Recommendations

Hydroacoustics is one of the best tools for examining the underwater environment at very high spatial and temporal resolutions. In tidal energy sites, it is one of the few tools that can be used to safely acquire information about fish. However, tidal energy sites also present unique challenges to acoustics sampling. The high-speed currents generate high levels of turbulence, which draw air into the water column and sometimes as far down as the seafloor. Backscatter from fish is completely masked within these contaminated areas. Much of this contamination can be identified and removed with a combination of automated steps (e.g. with the threshold offset line method in Echoview) and manual scrutiny (corrections to automated line detections). However, the appearance of this air in the echograms can change substantially, from easily defined "spikes" extending down from the surface, to nebulous clouds that appear mid-water-column. The timing and extent of entrained air contamination is difficult to predict, and thus far can only be removed by hand according to the judgement of the human observer. There is a distinct need for tools to help automate this process and reduce subjectivity, particularly in long-term datasets (e.g., the stationary dataset presented here). Machine learning is an active area of research in the acoustics community, and these techniques should be explored for applications at tidal energy sites.

Additional acoustic frequencies could also improve our ability to identify and separate fish from entrained air. In this dataset, we only had one frequency to work with, and therefore could not examine the frequency response of any of the scatterers. The frequency response could be useful for separating groups of interest—e.g., bubble clouds vs. fish schools [30]. This will depend on the size and density of the bubbles entrained into the water column and which species of fish are present, and therefore needs to be tested on site. Testing could be carried out from a vessel or a platform, as long as a wide range of noise types can be sampled concurrently (or nearly so) with the different frequencies.

Further assessment of the full mobile dataset is recommended in order to better understand the spatial structure of backscatter (fish presence and density) at this tidal energy site, and to be able to estimate the representative spatial range of acoustic data collected from a stationary platform. Data from just one transect was used here, as it was the closest to the stationary platform. However, results from this transect were inconclusive. Incorporating data from the other transects may help determine if this was an issue of resolution or span, and/or if the site simply exhibits no coherent spatial structure at the scales we are able to measure—i.e. if it is too tumultuous for fish to form any coherent spatial distribution during the running tide. At this stage, we have only scratched the surface and cannot say which is more likely.

The data from the stationary platform were incredibly useful in quantifying the temporal variability in backscatter measurements at this site. This dataset revealed a huge amount of temporal variability occurring over short time scales (seconds to hours), including strong

tidal and diel periodicities throughout the year. The magnitude of this variability was similar to or greater than the changes occurring at the seasonal scale. This finding agrees with previous assessments here and at other sites [12,26], and supports the continued use of 24-hr sampling in the mobile surveys. A 24 hr survey allows the tidal and diel variation in backscatter to be quantified, and the 24-hour average is more useful for tracking the longer term trends of interest (e.g., long-term changes in fish backscatter as an indicator of turbine effects). All three stationary datasets indicated the representative temporal range of a 24-hr mobile survey is approximately 3 days at the location sampled.

The goals of this assessment were primarily related to comparing the stationary and mobile datasets, and using their complementary information to determine the spatial or temporal applicability of the results from each. However, there is a wealth of biological information that could be extracted from these data, if challenges such as the identification and removal of noise, and the resulting varying quality and coverage of the data, can be addressed.

Budget

Please see separate MS Excel file.

Employment Summary

Please see section entitle ‘Performance measures’ below.

Bibliography

[1] Copping, A., Sather, N., Hanna, L., Whiting, J., Zydlewski, G., Staines, G., Gill, A., Hutchison, I., O'Hagan, A., Simas, T., Bald, J., Sparling, C., Wood, J., Masden, E. (2016). Annex IV 2016 State of the Science Report: Environmental Effects of Marine Renewable Energy Development Around the World. Richland, WA: Pacific Northwest National Laboratory. Available: http://tethys.pnnl.gov/publications/state-of-the-science-2016.

[2] Keyser, F.M., Broome, J.E., Bradford, R.G., Sanderson, B., & Redden, A.M. (2016). Winter presence and temperature-related diel vertical migration of Striped Bass (Morone saxatilis) in an extreme high flow site in Minas Passage, Bay of Fundy. Canadian Journal of Fisheries and Aquatic Science. DOI: 10.1139/cjfas-2016-0002.

[3] Stokesbury, M.J.W., Logan-Chesney, L.M., McLean, M.F., Buhariwalla, C.F., Redden, A.M., Beardsall, J.W., Broome, J.E., Dadswell, M.J. (2017). Atlantic sturgeon spatial and temporal distribution in Minas Passage, Nova Scotia, Canada, a region of future tidal energy extraction. PLoS ONE, vol 11, no 7, e0158387.

[4] Horne, J.K., Jacques, D.A., Parker-Stetter, S.L., Linder, H.L., and Nomura, J.M. (2013). Evaluating Acoustic Technologies to Monitor Aquatic Organisms at Renewable Energy Sites. National Ocean Partnership Program – Bureau of Ocean and Energy Management, Department of Energy. Final Report. 111 pp.

[5] Viehman, H.A., Zydlewski, G.B., McCleave, J., Staines, G. (2015). Using acoustics to understand fish presence and vertical distribution in a tidally dynamic region targeted for energy extraction. Estuaries and Coasts, vol 38, suppl 1, pp S215-S226.

[6] Staines, G., Zydlewski, G.B., Viehman, H., Shen, H., McCleave, J. (2015). Changes in vertical fish distributions near a hydrokinetic device in Cobscook Bay, Maine, USA. Proceedings of the 11th European Wave and Tidal Energy Conference. September 6-11 2015. Nantes, France.

[7] Bradley, P.T., Evans, M.D., Seitz, A.C. (2015) Characterizing the juvenile fish community in turbid Alaskan rivers to assess potential interactions with hydrokinetic devices. Transactions of the American Fisheries Society 144: 1058-1069.

[8] Seitz, A.C., Moerlein, K., Evans, M.D., Rosenberger, A.E. (2011) Ecology of fishes in a high-latitude, turbid river with implications for the impacts of hydrokinetic devices. Reviews in Fish Biology and Fisheries 21: 481-496.

[9] Redden, A.M., Stokesbury, M.J.W., Broome, J.E., Keyser, F.M., Gibson, A.J.F., Halfyard, E.A., McLean, M.F., Bradford, R. Dadswell, M.J., Sanderson, B., and Karsten, R. (2014). Acoustic tracking of fish movements in the Minas Passage and FORCE Demonstration Area: Pre-turbine Baseline Studies (2011-2013). Final Report to the Offshore Energy Research Association of Nova Scotia and Fundy Ocean Research Centre for Energy. Acadia Centre for Estuarine Research Technical Report No. 118, Acadia University, Wolfville, NS. 153p

[10] Baker, M., Reed, M., & Redden, A.M. (2014). Temporal Patterns in Minas Basin Intertidal Weir Fish Catches and Presence of Harbour Porpoise during April – August 2013. ACER, Wolfville, NS, Technical Report 120.

[11] Dadswell, M.J. (2010). Occurrence and migration of fishes in Minas Passage and their potential for tidal turbine interaction. BioIdentification Associates. Technical Report. 35 pp.

[12] Viehman, H.A., Boucher, T., & Redden, A.M. (2018). Winter and summer differences in probability of fish encounter with MHK devices. International Marine Energy Journal, vol 1, no 1.

[13] Horne, J.K. (2000). Acoustic approaches to remote species identification: a review. Fisheries Oceanography, vol 9, no 4, pp 356-371.

[14] Simmonds, J., MacLennan, D.N. (2005). Fisheries acoustics: theory and practice. Oxford: Blackwell.

[15] Daroux, A. & Zydlewski, G.B. (2017). Final Report 2016-2017 Mobile Acoustic Fish Monitoring of the Fundy Ocean Research Center Crown Lease Area. Report submitted to the Fundy Ocean Research Center for Energy.

[16] Horne, J.K., and Jacques, D.A. (2018). Determining representative ranges of point sensors in distributed networks. Environmental Monitoring Assessment, vol 190, no 348.

[17] Jacques, D. (2014). Describing and comparing variability of fish and macrozooplankton density at marine hydrokinetic energy sites. M. Sc. Thesis, University of Washington.

[18] Melvin G.D. & Cochrane, N.A. (2014). Investigation of the vertical distribution, movement and abundance of fish in the vicinity of proposed tidal power energy conversion devices. Final Report submitted to Offshore Energy Research Association (OERA), Research Project 300-170-09-12.

[19] Shen, H., Zydlewski, G.B., Viehman, H.A., & Staines, G. (2016). Estimating the probability of fish encountering a marine hydrokinetic device. Renewable Energy, vol 97, pp 746-756. DOI: 10.1016/j.renene.2016.06.026.

[20] Lieber, L., Nimmo-Smith, W.A.M., Waggitt, J.J., Kregting, L. (2018) Fine-scale hydrodynamic metrics underlying predator occupancy patterns in tidal stream environments. Ecological Indicators, vol 94, pp 397-408. https://doi.org/10.1016/j.ecolind.2018.06.07

[21] Scherelis, C., Penesis, I., Marsh, P., Cossu, R., Hemer, M., Write, J. (2019) Relating fish distributions to physical characteristics of a tidal energy candidate site in the Banks Strait, Australia. Proceedings of the 13th European Wave and Tidal Energy Conference. 1-6 Sept 2019, Naples, Italy.

[22] Fraser, S., Nikora, V., Williamson, B.J. & Scott, B.E. (2017). Automatic active acoustic target detection in turbulent aquatic environments. Limnology and Oceanography, vol 15, no 2, pp 184-199. DOI: 10.1002/lom3.10155.

[23] Wiesebron, L.E., Horne, J.H., & Hendrix, A.N. (2016). Characterizing biological impacts at marine renewable energy sites. International Journal of Marine Energy, vol 14, pp 27-40. DOI: 10.1016/j.ijome.2016.04.002.

[24] Wiesebron, L.E., Horne, J.K., Scott, B.E., & Williamson, B.J. (2016). Comparing nekton distributions at two tidal energy sites suggests potential for generic environmental monitoring. International Journal of Marine Energy, vol 16, pp 235-249. DOI: 10.1016/j.ijome.2016.07.004.

[25] Williamson, B.J., Fraser, S., Blondel, P., Bell, P.S., Waggitt, J.J. & Scott, B.E. (2017). Multisensor Acoustic Tracking of Fish and Seabird Behavior Around Tidal Turbine Structures in Scotland. IEEE Journal of Oceanic Engineering. DOI: 10.1109/JOE.2016.2637179.

[26] Viehman, H.A. & Zydlewski, G.B. (2017). Multiscale temporal patterns in fish presence in a high-velocity tidal channel. PLoS ONE, vol 12, no 5. DOI: 10.1371/journal.pone.0176405.

[27] Urmy, S.S., Horne, J.K., Barbee, D.H. (2012). Measuring the vertical distributional variability of pelagic fauna in Monteray Bay. ICES Journal of Marine Science, vol 69, no 2, pp 184-196.

[28] Urmy, S.S., Horne, J.K. (2016). Multi-scale responses of scattering layers to environmental variability in Monterey Bay, California. Deep-Sea Research I, vol 113, pp 22-32.

[29] Demer, D.A., Berger, L., Bernasconi, M., Bethke, E., Boswell, K., Chu, D., Domokos, R., et al. (2015). Calibration of acoustic instruments. ICES Cooperative Research Report No. 326. 130 pp.

[30] Korneliussen, R. J. (Ed.). (2018). Acoustic target classification. ICES Cooperative Research Report No. 344. 104 pp. http://doi.org/10.17895/ices.pub.4567

[31] Mackenzie, K. V. (1981). Nine-term equation for sound speed in the ocean. Journal of the Acoustical Society of America, vol 70, pp 807-12. https://doi.org/10.1121/1.386920

[32] Leroy, C. C. (1969). Development of simple equations for accurate and more realistic calculation of the speed of sound in sea water. Journal of the Acoustical Society of America, vol 46, pp 216-26.

[33] Ryan, T.E., Downie, R.A., Kloser, R.J., Keith, G. (2015). Reducing bias due to noise and attenuation in open-ocean echo integration data. ICES Journal of Marine Science. doi: 10.1093/icesjms/fsv121.

[34] Benoit-Bird, K. J., Southall, B. L., Moline, M.A. (2019). Dynamic foraging by Risso's dolphins revealed in four dimensions. Marine Ecology Progress Series, vol 632, pp 221-234.

[35] Hartman, K.J., Nagy, B.W. (2005). A target strength and length relationship for striped bass and white perch. Transactions of the American Fisheries Society, vol 134, pp 375-380. DOI: 10.1577/T04-052.1.

[36] R Core Team (2019). R: A language and environment for statistical computing. R Foundation for Statistical Computing, Vienna, Austria. https://www.R-project.org/.

[37] "Water Quality Monitoring: Conductivity to Salinity Conversion." Fivecreeks.org. Friends of Five Creeks. Accessed December 2019. <http://www.fivecreeks.org/monitor/sal.shtml>

[38] Francois, R.E., and Garrison, G.R. (1982). Sound absorption based on measurements. Part II: Boric acid contribution and equation for total absorption. Journal of the Acoustical Society of America, vol 72, pp 1879-90. https://doi.org/10.1121/1.388673

[39] Fletcher, R,. and Fortin, M. (2018). Spatial ecology and conservation modelling: applications with R. Switzerland: Springer.

[40] Ribeiro Jr, P.J., and Diggle, P.J. (2018). geoR: Analysis of Geostatistical Data. R package version 1.7-5.2.1. https://CRAN.R-project.org/package=geoR

[41] Holmes, E. E., Scheuerell, M.D., and Ward, E.J. (2019) Applied time series analysis for fisheries and environmental data. NOAA Fisheries, Northwest Fisheries Science Center, 2725 Montlake Blvd E., Seattle, WA 98112. Contacts eli.holmes@noaa.gov, eric.ward@noaa.gov, and mark.scheuerell@noaa.gov

[42] Wilson, B., Batty, R.S., and Dill, L.M. (2004). Pacific and Atlantic herring produce burst pulse sounds. Proceedings of the Royal Society of London B, vol 271(suppl.), pp S95-S97.

[43] Pittman, S.J., McAlpine, C.A. (2001). Movements of marine fish and decapods crustaceans: process, theory and application. Advances in Marine Biology, vol 44, pp 205-294.

[44] Reebs, S.G. (2002). Plasticity of diel and circadian activity rhythms in fishes. Reviews in Fish Biology and Fisheries, vol 12, pp 349-71.

[45] Huse, I., Korneliussen, R. (2000). Diel variation in acoustic density measurements of overwintering herring (*Clupea harengus L*.). ICES Journal of Marine Science, vol 57, pp 903-10.

[46] Glass, C.W., Wardle, C.S., Mojsiewicz, W.R. (1986). A light intensity threshold for schooling in the Atlantic mackerel, *Scomber scombrus*. Journal of Fish Biology, vol 29(suppl. A), pp 71-81.[47]Maunder, M.N., Punt, A.E. (2004). Standardizing catch and effort data: a review of recent approaches. Fisheries Research, vol 70, pp 141-59.

Performance measures (NR-Can)

1. Brief summary (1/2 page) of methodology – that can be taken directly from the Final Report.

   This project utilized hydroacoustic data collected during five 24-hr mobile surveys and three long-term stationary deployments of a bottom-mounted echosounder at the FORCE test site (December 2017 – November 2019) to evaluate the scientific and operational utility of individual and integrated hydroacoustic survey methods. Mobile surveys were conducted across a series of standardized transects of the FORCE test site from a vessel using a downward facing, pole-mounted Simrad EK80 WBT echosounder with a 7° circular split-beam transducer (i.e., 120 kHz in narrowband continuous wave (CW) mode). Stationary surveys included the deployment of an upward-facing Simrad EK80 Wideband Autonomous Transceiver (WBAT) with a circular beam transducer (i.e., half-power beam angle of 7°; 120 kHz in narrowband CW mode), and a Nortek Signature 500 ADCP mounted on a Fundy Advanced Sonar Technology autonomous subsea platform (i.e., FAST-3) that was deployed at the FORCE test site. Data processing was conducted using Echoview® software (version 10.0; Myriax, Hobart, Australia) and consisted of calibration, noise removal (i.e., minimum volume backscatter: -70 dB re 1 m^2 m^{-3}), data partitioning and echo integration. After processing, data were partitioned into bins, echo integrated, and exported for analyses. Analyses of mean volume backscatter (i.e., S_V – a rough index of fish density) or the area backscattering coefficient (i.e., s_a – the summation of backscatter values over a given layer in the water column; a complementary index of fish density) was conducted using the R statistical programming language (v3.6.2; R Core Team 2019). Analyses of mean S_V was used to asses spatial and temporal trends in water column backscatter, whereas analyses of s_a was used to assess the vertical distribution of backscatter through the water column. Spatial and temporal autocorrelation in the hydroacoustic data sets was assessed to determine the distance and time frame over which information from point measurements may be considered representative.

2. Key project achievements. These can be considered relevant to tidal development in general. eg. How your research has contributed to 'reducing uncertainty and investment risk for TEC devices and how it has contributed to further advancing the tidal energy industry; and/or contributions to building the supply chain for the sector, that could lead to global market use; reducing GHGs; etc.

   This project provided the first *in-situ* assessment of the relative performance of mobile (downward-facing) and stationary (upward-facing) echosounders for monitoring fish in high-flow environments. This project demonstrated the influence of high-flow environments on the ability of current hydroacoustic technologies to monitor interactions between fish and tidal energy turbines. Specifically, the primary achievements for this project include a deeper understanding of how dynamic forces in high flow environments (e.g., flow and bathymetry, turbulence and entrained air in the water column) combine to influence the efficacy of standard, commercially available, off-the-shelf hydroacoustic technologies for monitoring fish in areas where tidal power development are sought. This is crucial for understanding the limitations of current monitoring technologies and for quantifying the risk of tidal power development to marine animals. This project also highlighted the

importance of 24-hr collection of monitoring data to capture the variability of fish density present during different tidal phases and the influence of diel migration on fish distribution.

3. Where applicable, how the key project achievements led to benefits to project 'stakeholders' and to Canada. For any 'expected benefits', how these will be achieved in the coming years; Or other benefits to the wider tidal energy community?

   The achievements of this project benefit project stakeholders and Canada by broadening our understanding of how to effectively monitor the potential environmental impacts of tidal energy turbines in dynamic marine environments. This helps to ensure the continued responsible development of the marine renewable energy sector in Canada by advancing our understanding of the risk posed to marine life. Moreover, this project helps advance monitoring capabilities and protocols, and assists in quantifying risks for the regulatory community.

4. # technology and/or knowledge products generated (this can include software development); or the overarching goal of an 'ocean forecasting system'

   The knowledge gained includes a deeper understanding of how to effectively monitor for interactions between tidal energy turbines and marine animals. This in turn has implications for future monitoring efforts and protocols, data analyses and reporting procedures.

5. ID key operational issues or other barriers/challenges AND how they were resolved;

   Staff turnover presented a challenge for this program. Specifically, the absence of continuity – from the inception of the project until completion – by a single principal investigator generated confusion about study objectives and timelines for those who were required to take on this project while it was already underway. This project also encountered challenges in human resources required for processing raw hydroacoustic data. This specific challenge was remedied by providing training opportunities for staff (HQP development) and prioritizing and allocating dedicated blocks of time for staff to process data for analyses.

6. Listing of 'knowledge dissemination' activities undertaken over the course of the project.

   Project overviews were provided in FORCE's quarterly and annual reports to regulators that are made available to the public. Further, this project was included in overviews of the suite of monitoring activities undertaken at FORCE and presented at regional, national, and international meetings, symposia, and conferences.

7. If applicable, explain how the presence of federal, provincial, or municipal policies had an impact on your project? Or impact of current and forecasted energy and/or carbon prices?

8. # codes, standards, regulations, policies impacted/implemented?

   The results of this work may alter the course of fish monitoring activities at the FORCE site. However, this needs to be weighed against the value of the data collected from mobile hydroacoustic surveys that FORCE has been conducting since 2016 before a determination can be made.

9. #IPs (licenses? patents? TMs) generated?

   N/A

10. How is the project expected to continue over the next 5-year period? Eg. next steps for tech development, regulatory improvement, government involvement, market development, other? And

    The results of this project may alter the course of FORCE's fish monitoring program. Specifically, future fish monitoring at FORCE may move away from mobile hydroacoustic surveys to multiple stationary platforms with upward looking echosounders to quantify interactions between marine animals and tidal energy turbines.

11. Potential for replication of project in coming years?

    Given the results of this study, it is reasonable to expect that it will be replicated on a larger spatial scale to confirm the findings of this project and to help guide the future of fish monitoring activities at FORCE.

12. Total number HQPs (ID. Degree level, Total #months on project, Mitacs supported?

    Dr. Haley Viehman – PhD (36 months) – MITACS supported Post-doctoral fellow (Acadia University)
    Dr. Dan Hasselman – PhD (18 months)
    Tyler Boucher – BSc, Ocean Technologist diploma; Nova Scotia Community College (36 months)
    Jessica Douglas – Ocean Technologist diploma; Nova Scotia Community College (20 months)
    Milli Sanchez – BSc (8 months)
    Jeremy Locke – MSc (4 months)

13. And the following **additional metrics where applicable……**

	At the end of project	**5 yrs after project end (predicted)**	**In the year 2030 (predicted)**	**In the year 2050 (predicted)**
Annual direct GHG savings (if applicable)/	**N/A**	**N/A**	**N/A**	**N/A**
Annual indirect GHG savings (if applicable)/	**N/A**	**N/A**	**N/A**	**N/A**
Technology readiness level (TRL)/	**Improved**	**N/A**	**N/A**	**N/A**
Direct economic impact (if applicable)/	**N/A**	**N/A**	**N/A**	**N/A**
Indirect economic impact (if applicable)/	**N/A**	**N/A**	**N/A**	**N/A**
Direct employment full-time equivalent - FTE (male%, female %)/	**2 (50%:50%)**	**2 (50%:50%)**	**N/A**	**N/A**
Indirect employment full-time equivalent (FTE)/	**N/A**	**N/A**	**N/A**	**N/A**